Calcium-permeable AMPA receptors mediate timing-dependent LTP elicited by 6 coincident action potentials at Schaffer collateral-CA1 synapses

Running title: Modulation of threshold t-LTP

Efrain A. Cepeda-Prado[1#], Babak Khodaie[1,3#], Gloria D. Quiceno[1], Swantje Beythien[1], Volkmar Leßmann[1,2,3,Δ,*], Elke Edelmann[1,2,3*]

[1]Institut für Physiologie, Otto-von-Guericke-Universität, Medizinische Fakultät, Leipziger Str. 44, 39120 Magdeburg, Germany

[2]Center for Behavioral Brain Sciences, Magdeburg, Germany

[3]OVGU International ESF-funded Graduate School ABINEP, Magdeburg, Germany

[#] shared first authorship, * Shared senior authorship

[Δ] correspondence: lessmann@med.ovgu.de

Keywords:

spike timing-dependent plasticity, STDP, hippocampus, dopamine, calcium, BDNF, t-LTP

Abstract

Activity-dependent synaptic plasticity in neuronal circuits represents a cellular model of memory formation. Such changes can be elicited by repeated high-frequency stimulation inducing long-term potentiation (LTP), or by low frequency stimulation induced long-term depression (LTD). Spike timing-dependent plasticity (STDP) can induce equally robust long-lasting timing-dependent LTP (t-LTP) in response to low frequency repeats of coincident action potential (AP) firing in presynaptic cells followed by postsynaptic neurons. Conversely, this stimulation can lead to t-LTD if the postsynaptic spike precedes the presynaptic action potential. STDP is best suited to investigate synaptic plasticity mechanisms at the single cell level. Commonly, STDP paradigms relying on 25-100 repeats of coincident pre- and postsynaptic firing are used to elicit t-LTP or t-LTD. However, the minimum number of repeats required for successful STDP induction, which could account for fast single trial learning *in vivo*, is barely explored. Here, we examined low repeat STDP at Schaffer collateral-CA1 synapses by pairing one presynaptic AP with either one postsynaptic AP (1:1 t-LTP) or a burst of 4 APs (1:4 t-LTP). We found 3-6 repeats to be sufficient to elicit t-LTP. Postsynaptic Ca^{2+} elevation for 1:1 t-LTP required NMDARs and L-type VGCCs, while 1:4 t-LTP depended on metabotropic GluR and ryanodine receptor signaling. Surprisingly, both 6x t-LTP variants were strictly dependent on activation of postsynaptic Ca^{2+}-permeable AMPARs. Both t-LTP forms were regulated differentially by dopamine receptors, but occurred independent from BDNF/TrkB signaling. Our data show that synaptic changes induced by only 3-6 repeats of mild STDP stimulation occuring in ≤10 s can take place on time scales observed also during single trial learning.

Introduction

Long-term potentiation (LTP) and long-term depression (LTD) of synaptic transmission can be observed in response to repetitive activation of synapses and are believed to represent cellular models of learning and memory processes in the brain (see e.g., Bi and Poo, 1998; Bliss and Cooke,

2011; Malenka and Bear, 2004). While LTP leads to a stable enhancement of synaptic transmission between connected neurons, LTD yields a long-lasting decrease in synaptic responses. Depending on the time frame that is investigated, LTP as well as LTD can be divided into an early phase lasting roughly 1h and a late phase that starts 2-3h after induction of the synaptic change. While early LTP is mediated by posttranslational modifications, late LTP was found to depend on synthesis of new proteins (Lynch, 2004; but see Wang et al., 2016). LTP was initially discovered using long-lasting high frequency stimulation of glutamatergic synapses in the mammalian hippocampus (Bliss and Lomo, 1973), a brain region essential for encoding episodic memory (Tonegawa et al., 2018). While in these pioneering studies, LTP was recorded *in vivo* using extracellular field potential recordings (Bliss and Lomo, 1973), LTP is also observed in acutely isolated brain slices *ex vivo* and can be recorded in individual neurons using whole cell patch clamp recording techniques (reviewed e.g. in Herring and Nicoll, 2016; Lalanne et al., 2018; Pinar et al., 2017). Notably, LTP studies at the single cell level are essential to understand the biochemical and cellular mechanisms of LTP and LTD processes of a specific neuronal connection with defined postsynaptic target. To relate results from LTP measurements in acute slices *ex vivo* with learning processes it is important to use LTP induction protocols that resemble synaptic activation patterns also occurring during memory formation *in vivo* (compare Bittner et al., 2015; 2017; Otto et al., 1991), rather than paradigms involving tetanic synaptic stimulation or long-lasting artificial depolarization of postsynaptic neurons.

In this respect, spike timing-dependent plasticity (STDP) seems to represent an especially relevant protocol for induction of LTP (e.g., Bi and Poo, 2001; Caporale and Dan, 2008; Costa et al., 2017; Edelmann et al., 2017; Edelmann et al., 2014; Feldman, 2012; Markram et al., 2011). Here, bidirectional plasticity can be induced by repeated coincident activation of pre- and postsynaptic neurons, with forward pairing (i.e. presynaptic spike occurs several ms before the postsynaptic action potential; positive spike timing (+Δt)) yielding timing-dependent (t-) LTP, while backward pairing (postsynaptic spike occurs before presynaptic activation; -Δt) yields t-LTD. These protocols also fulfill the prerequisites for Hebbian synaptic plasticity (Caporale and Dan, 2008) that are widely accepted as fundamental requirements for synaptic plasticity. Compared to pairing protocols that induce LTP

by combining a presynaptic tetanus with a postsynaptic depolarization (e.g., Meis et al., 2012), STDP relies on a small number of pre- and postsynaptic action potentials that are repeated at low frequency (< 5 Hz).

Like memory formation *in vivo*, t-LTP in acute *ex vivo* brain slices is strongly controlled by neuromodulatory inputs, which can regulate the efficacy of induction paradigms to elicit plasticity (Edelmann and Lessmann, 2011, 2013; reviewed in Edelmann and Lessmann, 2018; Liu et al., 2017; Pawlak and Kerr, 2008; e.g., Seol et al., 2007). Such kind of neuromodulation can also bridge the temporal gap between synaptic plasticity and behavioral time scales for learning processes (Gerstner et al., 2018; Shindou et al., 2019), to connect synaptic effects to behavioral readouts. T-LTP was also reported to depend on brain-derived neurotrophic factor signaling (e.g., Edelmann et al., 2015; Lu et al., 2014; Mu and Poo, 2006; Pattwell et al., 2012; Sivakumaran et al., 2009). Still, these mechanistic studies on t-LTP employed STDP protocols depending typically on 25-100 repeats at ≤1 Hz that are unlikely to occur at synapses during memory formation *in vivo*. Therefore, in the present study we started out to determine the minimum number of repeats of coincident activation of pre- and postsynaptic neurons required for successful t-LTP induction. To this aim, we used low repeat variants of our recently described canonical (1:1 pairing: Edelmann and Lessmann, 2011) and burst STDP protocols (1:4 pairing: Edelmann et al., 2015; Solinas et al., 2019). Although, STDP protocols involving low repeat synaptic activation have been used previously to induce t-LTP (somatosensory cortex: Cui et al., 2015; Cui et al., 2016; visual cortex: Froemke et al., 2006; cultured hippocampal cells: Zhang et al., 2009), the underlying cellular mechanisms for its induction and expression remained elusive.

Our present study demonstrates that Schaffer collateral (SC)- CA1 t-LTP can be induced robustly by only three to six repeats of coincident pre- and postsynaptic spiking at 0.5 Hz. Moreover, our study reveals that, depending on specific STDP paradigms (i.e. 1:1 vs. 1:4) the low repeat protocols recruit distinct sources for postsynaptic Ca^{2+} elevation during induction of t-LTP, are mediated by distinct pre- and postsynaptic expression mechanisms, and are differentially regulated by dopamine receptor signaling. Together these data suggest that hippocampal SC-CA1 synapses can recruit multiple types

of synaptic plasticity in response to low repeat STDP protocols for processing of information and memory storage in the hippocampus. Altogether, these distinct cellular STDP pathways might form the basis for the pluripotency of hippocampal functions in learning and memory.

Results

Timing-dependent LTP at Schaffer collateral-CA1 synapses requires 3-6 spike pairings

Using whole cell patch clamp recordings, we investigated timing-dependent (t-)LTP at Schaffer collateral (SC) -CA1 synapses in acute hippocampal slices obtained from juvenile (i.e. P28-35) male C57BL/6J mice. T-LTP was induced by STDP protocols consisting of low repeat coincident pre- and postsynaptic action potentials at low pairing frequencies (0.5 Hz).

SC-CA1 synapses were repeatedly activated by pairing of an excitatory postsynaptic potential (EPSP) that was elicited by supra-threshold extracellular SC stimulation, with a single postsynaptically evoked action potential (AP; 1EPSP/1AP or 1:1, Δt= 10 ms at 0.5 Hz; compare **Fig. 1A**). To determine the minimal repeat number required for successful t-LTP induction with a prototypical STDP paradigm, neurons were subjected to either 70, 25, 6, or 3 repeats of single spike pairings. Unexpectedly, we found that just six spike pairings with 1:1 stimulation delivered at a frequency of 0.5 Hz were sufficient to induce robust potentiation of EPSP slopes to 154.5 ± 8.2% at 30 min after induction. The t-LTP magnitude was similar to the respective magnitude of t-LTP induced with either 25 or 70 repeats and significantly different from negative controls (25 x: 145.4 ± 9.1% and 70 x: 166.9 ± 11.8 %; ANOVA $F_{(4,114)}$=4,8562 p=0.0012, STDP experiments performed with 3 x 1:1 stimulation at 0.5 Hz, showed only a very slight average increase of EPSP slopes to 104.6 ± 22.5% 30 min after induction that was highly variable between cells. The average value was not significantly different from the respective EPSP slopes observed after 40 min in control neurons that were not subjected to STDP stimulation (negative controls (0:0): 105.0 ± 6.5%; **Fig. 1A**). The time course of changes in synaptic strength in an individual cell that was potentiated with the low repeat 1:1 protocol is depicted at the right side in blue. These data indicate that t-LTP can be induced at SC-CA1 synapses

with low repeat t-LTP paradigms (i.e. 6 x 1:1), that might more closely resemble the natural pattern of pre- and postsynaptic activity that can be observed during memory formation in CA1 *in vivo* than any high frequency or high repeat LTP protocol.

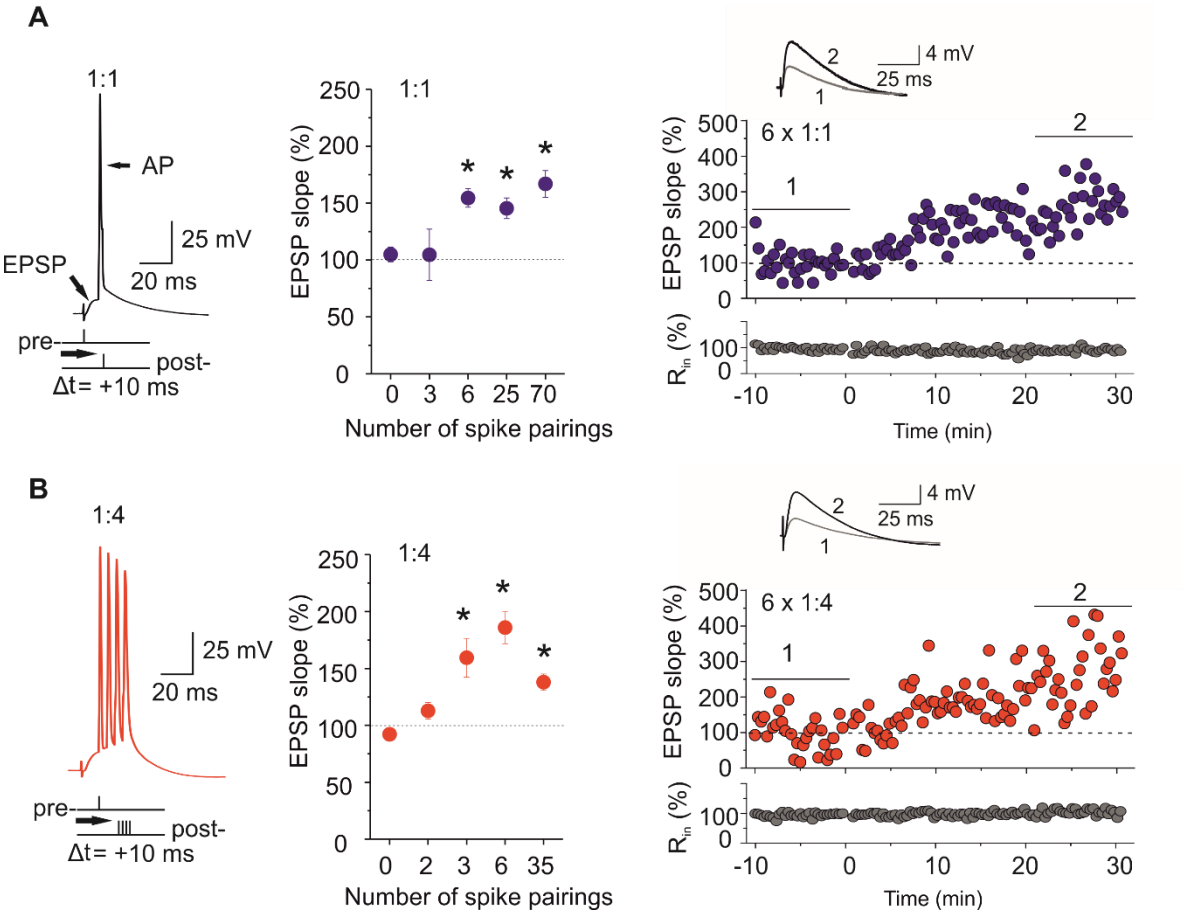

Figure 1: Low repeat t-LTP at Schaffer collateral-CA1 synapses is dependent on stimulation pattern and on the repeat number. A) *1:1 t-LTP protocol consisting of the temporal coincident stimulation of an EPSP and one postsynaptic action potential (AP) with a time delay of +10 ms. Summary plot showing the average magnitude of t-LTP (EPSP slope normalized to baseline recording) in response to variable numbers of repeats of the 1:1 t-LTP protocol delivered at 0.5 Hz. Successful t-LTP could be induced with 6 (n= 56 / N= 44), 25 (n= 26 / N= 6) and 70 (n=10 / N=7) repeats of the 1:1 t-LTP protocol. Three repeats did not cause any changes in synaptic strength (n=7 / N=6), and showed similar normalized EPSP slopes as negative controls (0:0; n=23 / N=17). Right: original EPSPs and time course of 6 x 1:1 induced potentiation recorded in an individual representative cell.* ***B)*** *1:4 t-LTP protocol consisting of the temporal coincident stimulation of an EPSP and four postsynaptic action potentials (APs) with a time delay of +10 ms. Summary plot showing the average magnitude of t-LTP (EPSP slope normalized to baseline recording) in response to variable numbers of repeats of the 1:4 t-LTP protocol delivered at 0.5 Hz. Successful t-LTP could be induced with 3 (n=10 /N= 3), 6 (n=10 / N=6)*

*and 35 (n=10 / N=8) repeats of the 1:4 t-LTP protocol. Two repeats did not cause changes in synaptic strength (n=10 /N =3) and showed similar normalized EPSP slopes as negative controls (0:0; n=7 / N=3). Right: original EPSPs and time course of 6 x 1:4 induced potentiation recorded in an individual representative cell. Averaged traces for EPSPs before and after LTP induction are shown as insets. * p < 0.05 ANOVA posthoc Dunnet's test. Data are shown as mean ± SEM.*

Since it has been suggested, that successful induction of t-LTP at SC-CA1 synapses requires firing of multiple postsynaptic APs (Buchanan and Mellor, 2007; Pike et al., 1999; Remy and Spruston, 2007), we incorporated a postsynaptic burst (4 APs delivered at 200 Hz) into the 6 x 1:1 protocol (**Fig. 1B**). This protocol is referred to as 6 x 1EPSP/4AP (or 6 x 1:4, **Fig. 1B**) paradigm and induced t-LTP at SC-CA1 synapses with the same efficiency as the 6 x 1:1 protocol (compare **Fig. 2C, D**). As for the canonical protocol, we determined the threshold number of repeats also for the burst protocol. As shown in **figure 1B**, successful 1:4 t-LTP could be induced by only three repeats of our burst protocol. Three (159.4 ± 15.9%), 6 (185.9± 14.2%) and 35 repeats (138.0 ± 7.1%) of 1:4 stimulation all yielded significant potentiation compared to the negative control (0 x repeats (92.2 ± 5.0%); ANOVA $F_{(4,42)}$=9.3654 p<0.0001, posthoc Dunnett's Test: 3 x: p=0.0017; 6 x: p<0.0001; 35 x: p=0.0415). The time course of change in synaptic strength of a typical cell obtained with 6 x 1:4 t-LTP stimulation is shown on the right. Since post-tetanic potentiation is lacking under these stimulation conditions, we observed for both t-LTP protocols a delayed onset (~5 min) and a subsequent gradual increase of t-LTP magnitude that typically proceeds until 30 min after induction, being consistent with previous t-LTP studies (compare e.g., Banerjee et al., 2009; Edelmann et al., 2015; Edelmann and Lessmann, 2011; Meredith et al., 2003; Nevian and Sakmann, 2006; Pattwell et al., 2012).

For further comparison and analysis of signaling and expression mechanisms of t-LTP we focused in all subsequent experiments on the 6 repeat protocols that induced with the same number of repeats successful t-LTP for both, the canonical and the burst paradigm (indicated as 6 x 1:1 or 6 x 1:4).

Canonical and burst containing low-repeat STDP paradigms induce Hebbian t-LTP

When spike pairings were delivered with longer time delays between pre- and postsynaptic firing (Δt: +20 ms) the magnitude of t-LTP declined (6 x 1:1: 132.1 ± 15.4% and 6 x 1:4: 118.3 ± 9.9%). Stimulation with short negative time delays (post-pre; Δt: -15 ms) did neither induce t-LTP nor significant t-LTD (6 x 1:1: 86.9% ± 9.6%; 6 x 1:4: 100.3 ± 9.8%; **Fig. 2A, B**).

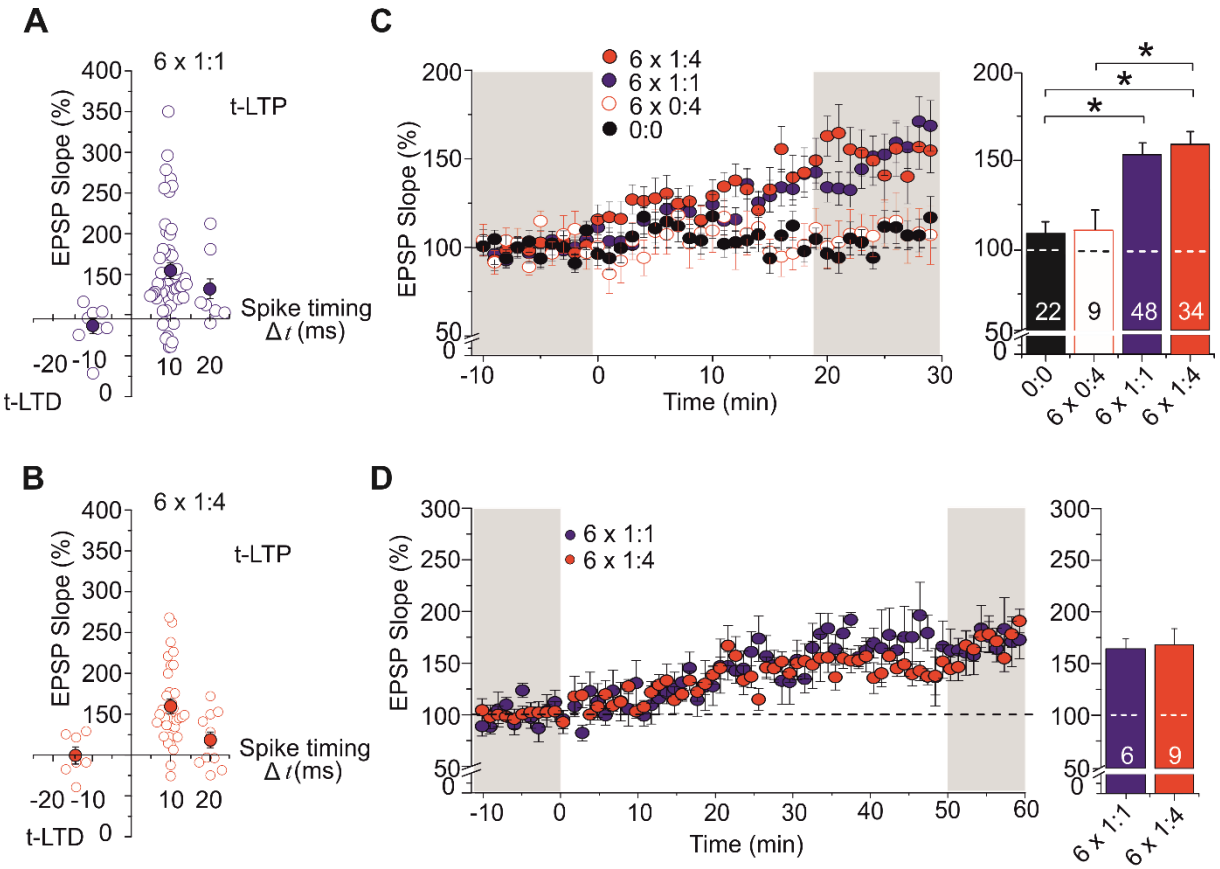

Figure 2: Comparison of canonical and burst low repeat STDP paradigms. *STDP plots for 6 x 1:1 (**A**, blue) and 6 x 1:4 (**B**, red) protocols. Changes in synaptic strength are shown for different intervals between start of the EPSP and postsynaptic APs. Groups of cells at +10 ms interval (standard), with longer time interval (+20 ms) or with negative spike pairings (-15 ms) are shown. Each open circle represents the result for an individual CA1 neuron. Mean values are shown as closed circles.* ***C)*** *The time courses of t-LTP expression did not differ between 6 x 1:1 (n= 48 / N= 44) and 6 x 1:4 (n=34 / N=27) paradigms, but they were significantly different from negative controls (0:0; n=22 / N=17) and unpaired controls (6 x 0:4; n=9 / N=7). The average magnitude of t-LTP is shown in the bar graphs.* ***D)*** *Extended measurements for 1 hour after t-LTP induction for both low repeat STDP protocols (6 x 1:1: n=6 / N=6, 6 x 1:4: n=9 / N=8). Data are shown as mean ± SEM, bar scales are shown in the insets.*

In general, the magnitude of t-LTP induced with the 6 x 1:4 stimulation (159.60 ± 8.00%) was comparable to that observed for 6 x 1:1 stimulation (153.65 ± 8.24%; $p > 0.05$, compare **Fig. 2C**). Eliciting only postsynaptic bursts without pairing to presynaptic stimulation (6 x 0:4; 110.08 ± 11.90%) did not yield significant potentiation compared to negative controls (0:0; 108.6 ± 7.11%, $p > 0.05$; **Fig. 2C**). Importantly, these results demonstrate that repeated postsynaptic burst firing alone does not induce any change in synaptic strength, indicating hebbian features for our low repeat t-LTP protocols, thereby delimiting our protocols from non-hebbian behavioral time scale synaptic plasticity recently reported for hippocampal places cells (Bittner et al., 2017). Prolonged patch clamp recordings carried out for 1 hour after pairing showed that both low repeat STDP paradigms yielded at 60 min comparable t-LTP magnitudes as observed 30 min after pairing. These data demonstrate that both low-repeat protocols enable longer lasting changes in synaptic transmission without any decline in magnitude. Moreover, the overall time course of the potentiation was indistinguishable for both types of low repeat t-LTP (**Fig. 2D**, potentiation after 1h: 6 x 1:1: 164.0 ± 9.5% and for 6 x 1:4: 168.0 ± 14.8%, $t_{(13)}$=-0.20435 p=0.84155). Together, these findings indicate that the low repeat STDP paradigms identified in this study induce Hebbian plasticity selectively at short positive spike timings with similar properties as have been described in earlier studies using high repeat canonical and burst type STDP protocols (e.g., Bi and Poo, 1998; Edelmann et al., 2015; Froemke et al., 2006).

In the next series of experiments, we determined the mechanisms of induction and expression as well as the intracellular signaling cascades involved in modulation of both types of low repeat t-LTP.

Influence of single and multiple postsynaptic action potentials on t-LTP expression

To investigate whether the low repeat STDP paradigms introduced here, rely on pre- or postsynaptic expression mechanisms of synaptic plasticity, we determined changes in the paired pulse ratio (PPR) before and 30 min after t-LTP induction that was obtained when two successively evoked EPSPs were elicited at 50 ms inter-stimulus interval (**Fig. 3A**). Commonly, a decrease in PPR after induction of LTP is interpreted as an increase in transmitter release probability and would be expected in case of

223 presynaptically expressed synaptic plasticity. When t-LTP was induced with the 6 x 1:1 paradigm we
224 found on average in fact a significant decrease in PPR (before: 1.91 ± 0.1, after: 1,7 ±0.1; paired
225 Student's t-test, $t_{(34)}$ =2.3471; p= 0.0249, whereas the PPR remained unchanged after inducing 6 x 1:4
226 t-LTP (before: 1.78 ± 0.13; after: 1.6 ± 0.1; paired Student's t-test, $t_{(20)}$ = 1.0146; p = 0.3224; for
227 negative controls: before: 1.77 ± 0.07, after: 1.80 ± 0.12; paired Student's t-test, $t_{(20)}$ = -0.3494; p =
228 0.7305; **Fig. 3A**). This decreased PPR after induction of 6 x 1:1 t-LTP hints at a presynaptic expression
229 mechanism. In contrast, the PPR analysis clearly speaks against any presynaptic contribution in the
230 expression of 6 x 1:4 t-LTP. Interestingly, the initial PPR before inducing t-LTP was not significantly
231 different between the tested groups (negative control (0:0): 1.77 ± 0.07; 6 x 1:1: 1.91 ± 0.1; 6 x 1:4:
232 1.78 ± 0.13; Kruskal-Wallis test, $H_{(2)}$ = 0.8503; p = 0.6537), indicating that the initial release
233 probability was similar and a stable basal parameter in our slices. As additional measures for a
234 presynaptic expression mechanism, we determined miniature EPSCs and coefficient of variation (CV)
235 analysis before and after successful induction of our 6x 1:1 t-LTP (**Fig. S1**, compare Bender et al.,
236 2009; Edelmann et al., 2015). The results of both types of analysis are consistent with presynaptic
237 expression of 6 x 1:1 t-LTP, as the overall mean for CV after LTP was decreased (before: 0.47 ± 0.02,
238 after: 0.39 ± 0.02, and miniature EPSC frequencies (determined as shorter inter event intervals (IEI))
239 were increased after 6 x 1:1 t-LTP induction (see **Fig. S1**).
240

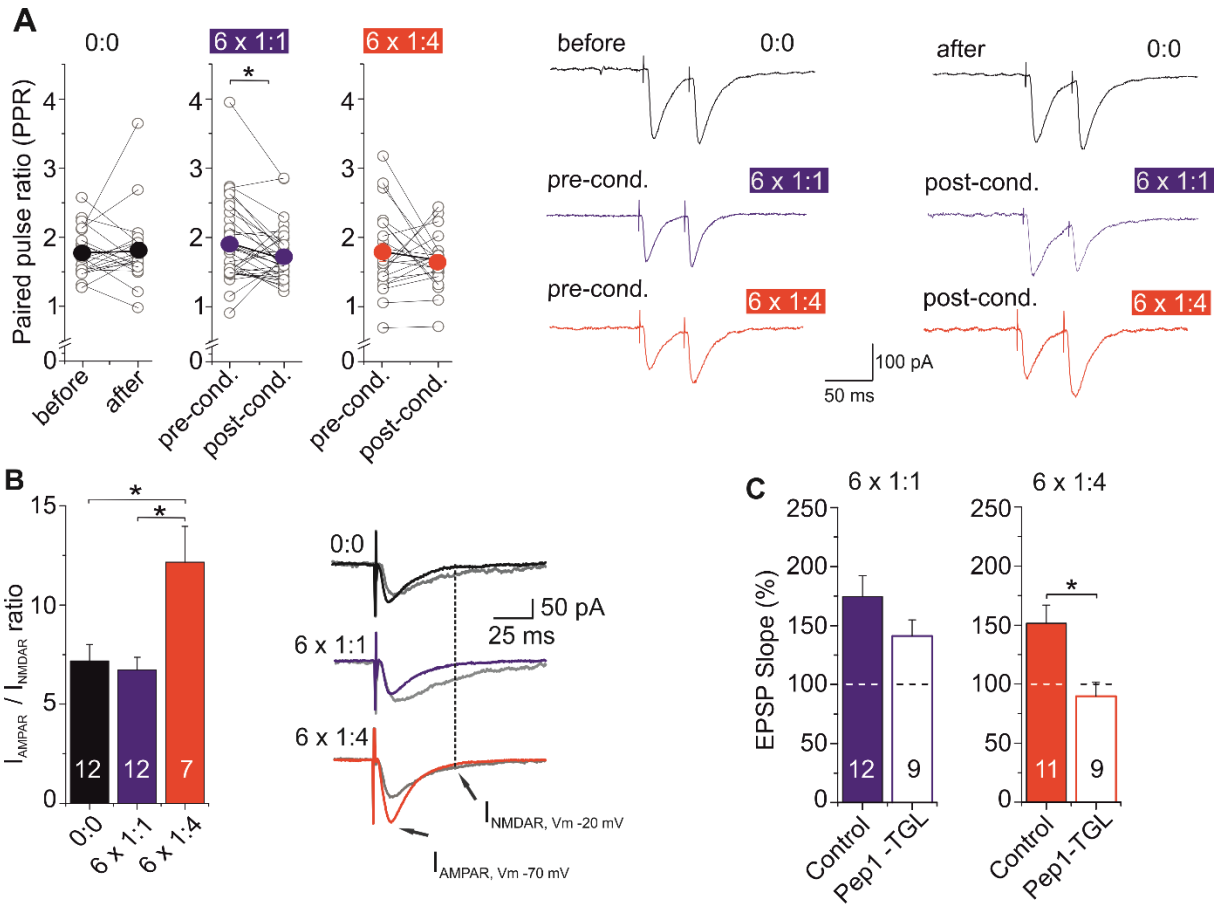

Figure 3: Different loci of expression for t-LTP induced by the low repeat 1:1 and 1:4 paradigms. A) *Paired pulse ratio (PPR) calculated before (pre-cond.) and 30 min after (post-cond.) t-LTP induction, or at the beginning and the end of measurements in negative controls (0:0: n=21 / N=6) and following t-LTP induction (6 x 1:1: n=35 / N=12; 6 x 1:4: n=21 / N=7).* ***B)*** *Right: original traces of AMPAR mediated currents recorded in voltage clamp at -70 mV holding potential (Vm) and NMDAR (gray) mediated currents at -20 mV holding potential. Left: ratio of AMPA/NMDA receptor mediated currents (AMPAR: peak current at -70 mV; NMDAR: current amplitude 50 ms after start of EPSC, recorded at -20 mV) for negative controls (0:0; n=12 / N= 9) and after induction of t-LTP with both low repeat paradigms (6 x 1:1: n= 12 / N=11; 6 x 1:4: n= 7 / N= 5).* ***C)*** *Intracellular application of Pep1-TGL (inhibiting membrane insertion of GluA containing AMPARs) via patch pipette blocked 6 x 1:4 t-LTP, whereas 6 x 1:1 t-LTP remained intact (6 x 1:1: ACSF; n= 12 / N= 10, Pep1-TGL n= 9 / N= 7 and 6 x 1:4: ACSF n= 11 / N= 11, Pep-TGL n= 9 / N= 7). Data are shown as mean ± SEM. Scale bars are shown in the figures.*

To further address the locus of expression of 6 x 1:1 and 6 x 1:4 t-LTP, we analyzed the changes in AMPA/NMDA receptor (R) mediated current ratios 30 min after inducing t-LTP. AMPAR mediated peak EPSCs were recorded at a holding potential of -70 mV, while NMDAR mediated current

components were determined as remaining current 50 ms after the peak EPSC recorded at -20 mV to avoid large current fluctuations of holding currents that are typically observed at positive membrane potentials. The AMPAR/NMDAR ratio analysis revealed a strong and statistically significant increase in AMPAR- vs. NMDAR-mediated excitatory postsynaptic currents (EPSCs) following the induction of 6 x 1:4 t-LTP but not when inducing 6 x 1:1 t-LTP, or in non-STDP stimulated control cells (0:0: 7.18±0.82, 1:1: 6.72 ± 0.65, 1:4: 12.15 ± 1.81; ANOVA $F_{(2, 34)}$ = 7.979; p = 0.0014, **Fig. 3B**). Since recording of NMDAR mediated currents at -20 mV (instead of +40 mV) results in smaller current amplitudes we might have introduced a larger error. However, since all groups (negative control, 6 x 1:1 and 6 x 1:4) were handled identically in this respect, the significant change specifically after t-LTP induction with 6 x 1:4 protocol, clearly points to a strong increase of postsynaptic AMPAR conductance, which is absent in the other groups. As an increase in AMPAR/NMDAR mediated currents after inducing LTP is commonly explained by the insertion of new GluA1 containing AMPARs into the postsynaptic spine (Chater and Goda, 2014; Edelmann et al., 2015; Lee and Kirkwood, 2011; Morita et al., 2014) these data strongly suggest a postsynaptic mechanism of expression selectively for the 6 x 1:4 t-LTP. Nevertheless, the AMPAR/NMDAR ratio can also be increased by postsynaptic mechanisms other than AMPAR receptor insertion (such as e.g. phosphorylation). Thus, we next investigated whether the 6 x 1:4 t-LTP is mediated specifically by incorporation of GluA1 containing AMPARs. To this aim, we loaded the postsynaptic cells with Pep1-TGL via the patch pipette solution and induced t-LTP with both 6 repeat t-LTP paradigms (compare Edelmann et al., 2015). Pep1-TGL contains the last three amino acids of the C-terminus of the GluA1 subunit, which are required for its insertion into the plasma membrane (Hayashi et al., 2000; Shi et al., 2001). The postsynaptic application of Pep1-TGL resulted in a complete block of 6 x 1:4 t-LTP (control: 151.42 ± 15.44, Pep1-TGL: 89.62 ± 11.92; Mann-Whitney U test, U = 14.0; p = 0.007). In contrast, t-LTP induced with the 6 x 1:1 protocol remained intact under the same recording conditions (control: 174.56 ± 17.86, Pep1-TGL: 141.13.71; Mann-Whitney U test, U = 36.0; p =0.201, **Fig. 3C**). Together with the PPR analysis and the AMPA/NMDAR ratios, these data suggest a dominant postsynaptic locus of expression for the 6 x 1:4 t-LTP. In contrast, the absence of any change in AMPA/NMDAR current ratio and AMPAR

insertion, in conjunction with the decreased PPR, decreased CV (paired student's t-test: $t_{(48)}$=4.5874; p< 0.0001), and increased mEPSC frequency (Kolmogorov-Smirnov 2sample test: Z=1.5745, p= 0.0132; compare **Fig. S1**) indicate a prevailing presynaptic locus of expression for the 6 x 1:1 t-LTP. These findings are consistent with our previous results obtained with high repeat t-LTP protocols (Edelmann et al., 2015). The data suggest that the number of postsynaptic spikes fired during induction of low repeat t-LTP decides whether associative Hebbian synaptic plasticity is expressed by pre- or by postsynaptic mechanisms, whereas the locus of t-LTP expression does not seem to depend on the number of repeats of a specific t-LTP paradigm.

Distinct calcium sources are recruited for induction of low repeat STDP paradigms

There is a general consensus that induction of long-lasting changes in synaptic strength at SC-CA1 synapses requires a postsynaptic rise in intracellular calcium concentration ($[Ca^{2+}]_i$) via NMDA receptors (NMDARs, Nicoll and Malenka, 1995). Likewise, also intracellular Ca^{2+} elevation resulting from synchronous activation of NMDARs, L-type voltage-gated Ca^{2+} channels (VGCC), and release of Ca^{2+} from internal stores, together with activation of metabotropic glutamate receptors (mGluRs) and subsequent activation of IP_3 receptors might be responsible for postsynaptic STDP induction (Tigaret et al., 2016). Accordingly, we investigated the sources for the intracellular Ca^{2+} elevation triggering the 6 x 1:1 and 1:4 t-LTP. Interestingly, the 6 x 1:1 t-LTP was significantly impaired when it was executed either in the presence of the specific NMDAR antagonist APV (50 µM; Control: 159.73 ± 15.23, APV: 110.91 ± 14.22; unpaired Student's t-test, $t_{(26)}$ = 2.348; p = 0.0268 ; **Fig. 4A**), or in the presence of the L-type VGCC blocker Nifedipine (25 µM; DMSO: 180.11 ± 17.32, Nifedipine: 90.19 ± 12.15; unpaired Student's t-test, $t_{(14)}$ = 4.25; p = 0.0008; **Fig. 4C**). In contrast, neither APV (50 µM, unpaired Student's t-test, $t_{(22)}$ = 1.016; p = 0.3207; **Fig. 4B**) nor Nifedipine (25 µM, Mann-Whitney U test, U = 20.0; p =0.6620, **Fig. 4D**) inhibited t-LTP induced with the 6 x 1:4 protocol (for 6 x 1:4: Control: 157.55 ± 19.71, APV: 137.95 ± 8.39 and DMSO: 159.75 ±10.81, Nifedipine: 171.73 ± 13.62). These data demonstrate that postsynaptic Ca^{2+} influx via NMDAR and L-type VGCC is required for 6 x 1:1 t-LTP but not for 6 x 1:4 t-LTP induction.

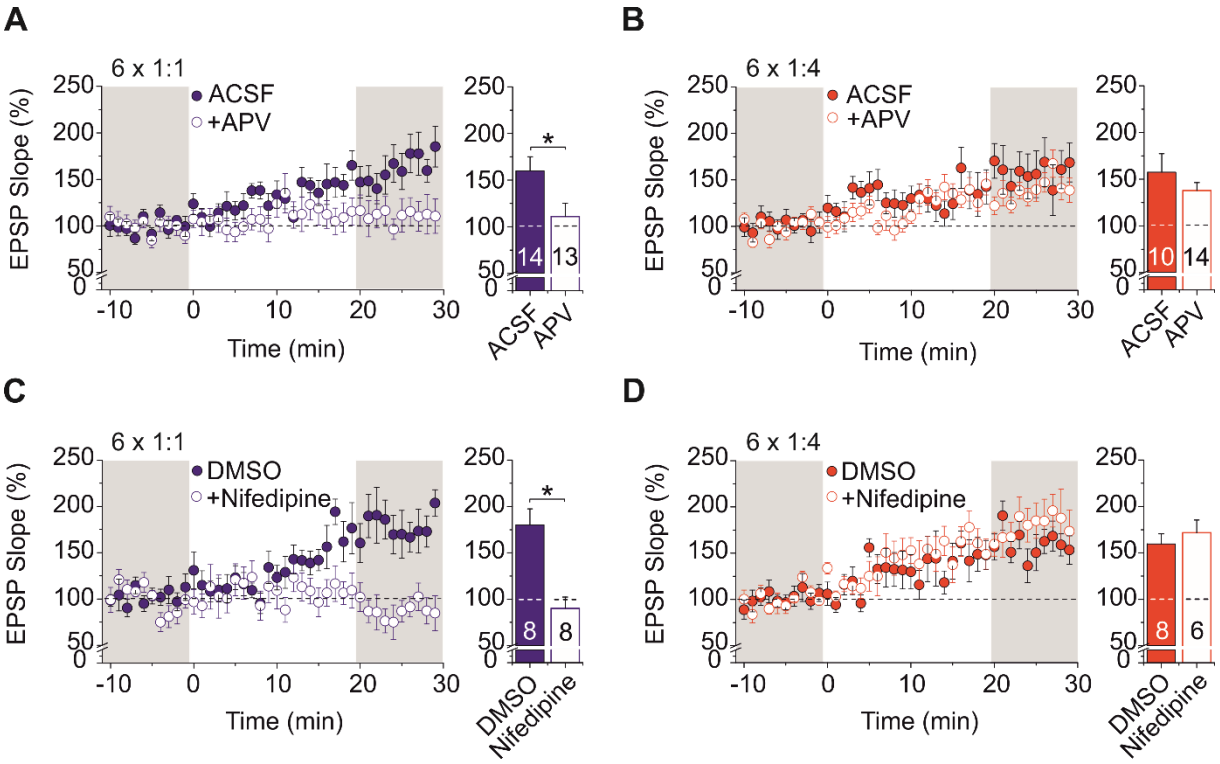

Figure 4: Contribution of NMDA receptors and VGCCs to the induction of 6 x 1:1 and 6 x 1:4 t-LTP. *Effects of bath applied NMDAR antagonist APV (50 µM) and L-type voltage-gated calcium channel (VGCC) inhibitor Nifedipine (25 µM) on low repeat t-LTP. Inhibition of either NMDARs* ***(A)*** *or L-type VGCCs* ***(C)*** *completely blocked 6 x 1:1 t-LTP (****A****: 6 x 1:1: ACSF n=14 / N=8, APV n= 13 / N= 12;* ***C****: DMSO control n= 8 / N=7, Nifedipine n=8 / N=7).* ***(B)*** *6 x 1:4 t-LTP remained unaffected by application of the NMDAR inhibitor APV (6 x 1:4: ACSF n=10 / N=6, APV n=14 / N=9).* ***D)*** *6 x 1:4 t-LTP was not inhibited in the presence of the L-type VGCC inhibitor nifedipine (DMSO n=8 / N=4, Nifedipine n=6 / N=4). Average time course of potentiation and mean (± SEM) magnitude of t-LTP are shown for the respective experiments.*

To verify a role of postsynaptic Ca^{2+} signaling in the induction of 6 x 1:4 t-LTP, we loaded postsynaptic neurons with 10 mM of the Ca^{2+} chelator BAPTA via the patch pipette solution (**Fig. 5A**). After obtaining the whole cell configuration, the BAPTA containing internal solution was allowed to equilibrate for 30 min before t-LTP induction. Likewise, in the respective control experiments t-LTP was also induced 30 min after breaking the seal. As shown in **figure 5A**, buffering of intracellular Ca^{2+}

signals with BAPTA resulted in a complete impairment of 6 x 1:4 t-LTP (Control: 150.28 ± 12.07, $BAPTA_i$: 104.80 ± 5.84; Mann-Whitney U test, U = 3.0; p =0.0303), indicating that a rise in postsynaptic $[Ca^{2+}]_i$ is indeed required also for the induction of 6 x 1:4 t-LTP.

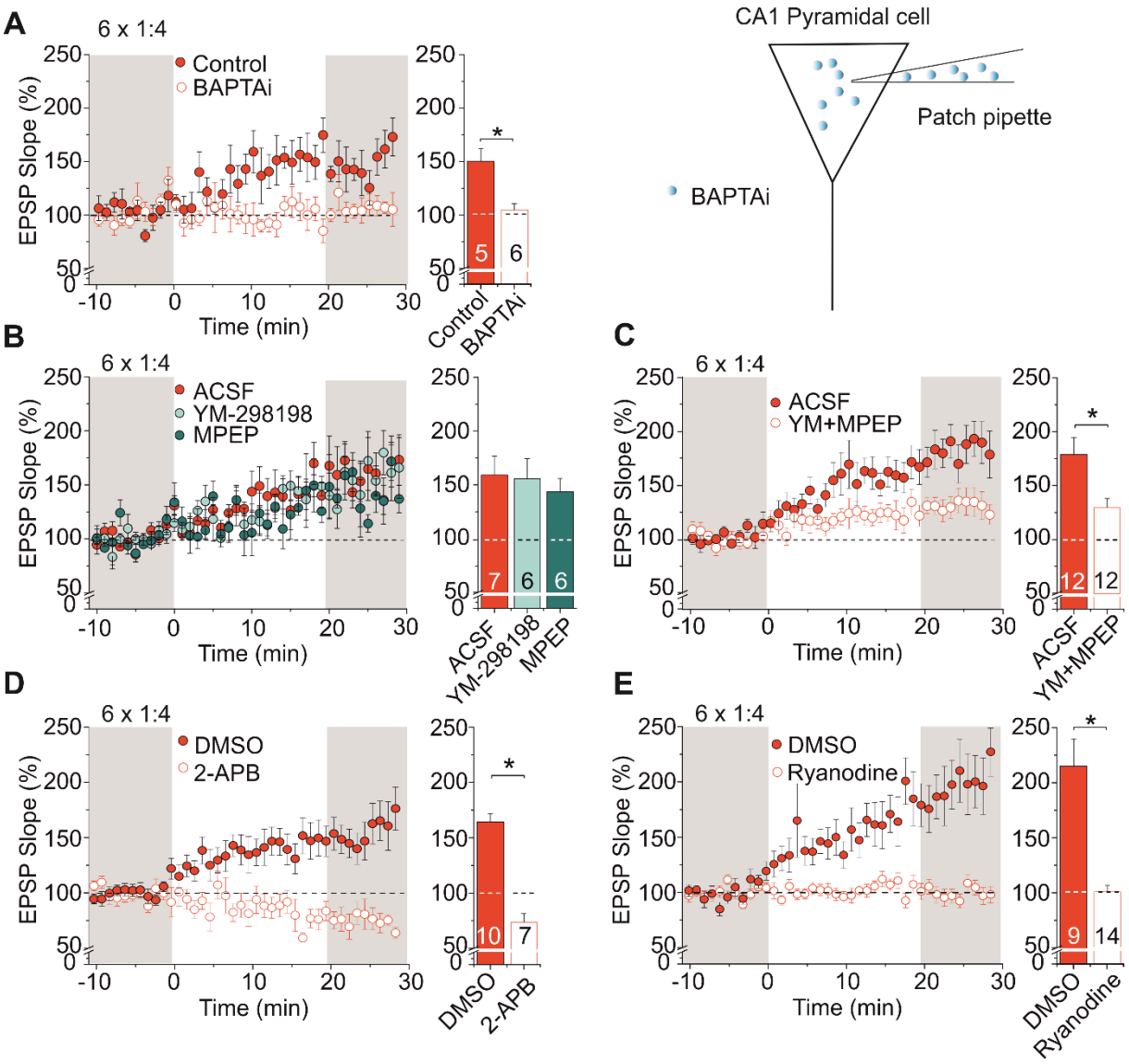

Figure 5: Contribution of group I mGluRs, IP3 receptors and ryanodine receptor-dependent calcium release from internal stores to 6 x 1:4 t-LTP. A) *Inclusion of 10 mM BAPTA in the pipette solution and equilibration with the cell interior for 30 min before t-LTP induction (open circles) prevented t-LTP induced by 6 x 1:4 stimulation compared to identically treated (i.e. t-LTP induction 30 min after breaking the patch) control cells (closed circles; Control: n=5 / N=5, $BAPTA_i$: n=6 / N=4), indicating the necessity of postsynaptic calcium elevation to induce t-LTP. The inset depicts the loading of the cell with BAPTA.* ***B)*** *T-LTP induced with the 6 x 1:4 protocol was neither affected by bath application of the mGluR1 antagonist YM-298198 (1 µM; ACSF: n=7 / N=5, YM-298198: n=6 / N=3), nor by the mGluR5 antagonist MPEP (10 µM, n=6 / N=4).* ***C)*** *However, co-application of both antagonists (YM-298198*

and MPEP; ACSF n=12 / N=8, YM-MPEP n=12 / N=5) significantly reduced synaptic potentiation. ***D)*** *Inhibition of IP3 receptors by 100 µM 2-APB (in 0.05% DMSO) completely blocked 6 x 1:4 t-LTP (DMSO n=10/ N=5; 2-APB n=7/ N=3).* ***E)*** *Wash in of 100 µM ryanodine into the postsynaptic neuron via the patch pipette inhibited t-LTP induced by 6 x 1:4 stimulation (DMSO n= 9 / N= 4; Ryanodine n= 14 / N= 5). Average time course of potentiation and mean (± SEM) magnitude of t-LTP are shown for the respective experiments.*

Since induction of t-LTP involves repeated glutamate release that, according to hebbian rules, should contribute to the induction process, we next tested the involvement of metabotropic glutamate receptors (mGluRs) in 6 x 1:4 t-LTP. In the hippocampal CA1 region $mGluR_1$ and $mGluR_5$ are widely expressed and have been reported to induce Ca^{2+} release from internal calcium stores during LTP (e.g., Balschun et al., 1999; Neyman and Manahan-Vaughan, 2008; Wang et al., 2016). Nevertheless, blocking mGluR activation by bath application of antagonists of either $mGluR_1$ (YM-298198 10 µM) or $mGluR_5$ (MPEP, 10 µM) alone, did not affect the magnitude of 6 x 1:4 t-LTP compared to ACSF controls (Control: 159.07 ±17.67; YM: 155.65 ± 18.70; MPEP: 143.51 ± 12.43; Kruskal-Wallis test, $H_{(2)}$ = 0.2774; p =0.8705; **Fig. 5B**). However, coapplication of the $mGluR_1$ and $mGluR_5$ antagonists significantly reduced the 6 x 1:4 t-LTP magnitude (Control: 178,99 ± 15.29; YM+MPEP: 129.97 ± 7.94; unpaired Student's t-test, $t_{(22)}$ = 2.248; p= 0.0093; **Fig. 5C**), indicating that the activation of one of these receptors alone (either $mGluR_1$ or $mGluR_5$) is sufficient and required to support 6 x 1:4 t-LTP. To investigate whether mGluR mediated Ca^{2+} release from internal stores contributes to 6 x 1:4 t-LTP we used 2-APB as an inhibitor of IP_3-receptors. As expected inhibition of IP_3-mediated Ca^{2+} release completely blocked t-LTP (DMSO: 164.30 ± 18.29; 2-ABP: 71.87± 7.54; unpaired Student's t-test, $t_{(15)}$=4.0297; p =0.0019, **Fig. 5D**).

To test for involvement of ER-resident ryanodine receptors (RyR) in the low repeat burst protocol, we applied 100 µM ryanodine (a concentration known to irreversibly inhibit RyR; Gao et al., 2005) via the patch pipette into the recorded postsynaptic neurons. As expected in case of RyR involvement, 6 x 1:4 t-LTP induction was completely inhibited under these conditions (DMSO: 216.21 ± 25.70; Ryanodine: 100.24 ± 5.07; Mann-Whitney U test, U= 5.5; p = 0.0003; **Fig. 5E**). These data

371 demonstrate that Ca^{2+} release from the ER is a critical component of 6 x 1:4 t-LTP. Thus, the
372 postsynaptic Ca^{2+} elevation required for induction of 6 x 1:4 t-LTP seems to involve $mGluR_1$ or $mGluR_5$
373 mediated release of Ca^{2+} from the ER via IP3 receptors and subsequent Ca^{2+} induced Ca^{2+} release via
374 RyRs.
375
376 **Distinct dopaminergic modulation of different low repeat t-LTP protocols at Schaffer collateral-CA1**
377 **synapses**
378 Dopamine (DA) serves as an important neuromodulator in learning and memory formation, as well in
379 synaptic plasticity mechanisms underlying both phenomena. DA receptors in the brain are classified
380 into two main families: D1-like receptors that include D1 and D5, and D2-like receptors that include
381 D2, D3 and D4 (Missale et al., 1998). It has been shown that activation of D1/D5 receptors has a
382 particularly strong influence on synaptic efficacy (e.g., Dubovyk and Manahan-Vaughan, 2018;
383 Papaleonidopoulos et al., 2018), and that treatment of cultured hippocampal neurons with
384 exogenous DA (20 µM) reduces the induction threshold for t-LTP from 60 to 10 spike pairings (Zhang
385 et al., 2009). To examine whether in our case, endogenous DA signaling is an essential component of
386 synaptic mechanisms triggering low repeat t-LTP, we investigated the effect of specific bath applied
387 antagonists for D1-like and D2-like DA receptors (D1: SCH23390 (SCH), 10 µM; D2: Sulpiride (Sulp), 10
388 µM). We found that t-LTP induced with 6 x 1:1 stimulation was blocked completely when SCH23390
389 and Sulpiride were coapplied (Control: 174.15 ± 15.26, SCH: 165.84 ± 18.03, Sulp: 136.23 ± 12.99,
390 SCH+Sulp: 93.02 ± 9.03; ANOVA $F_{(3,36)} = 6.2519$; $p = 0.0016$, posthoc Tukey -test for ACSF vs SCH+Sulp
391 $p= 0.0015$ and for SCH vs SCH+Sulp: $p= 0.0091$), whereas application of either the D1-like or the D2-
392 like receptor antagonist alone did not significantly reduce the magnitude of the 6 x 1:1 t-LTP (**Fig.**
393 **6A**). In contrast, the 6 x 1:4 t-LTP was dependent exclusively on D2-like receptor signaling, as was
394 evident from complete inhibition of this burst t-LTP in the presence of Sulpiride (significantly
395 different from ACSF controls; Kruskal-Wallis test $H_{(3)} = 12.65$; $p = 0.005$, **Fig. 6B**), whereas SCH23390
396 was without effect (Control: 147.51 ± 8.25, SCH: 153.64 ± 14.47, Sulp: 102.34 ± 12.25, SCH+Sulp:
397 108.67 ± 9.17).

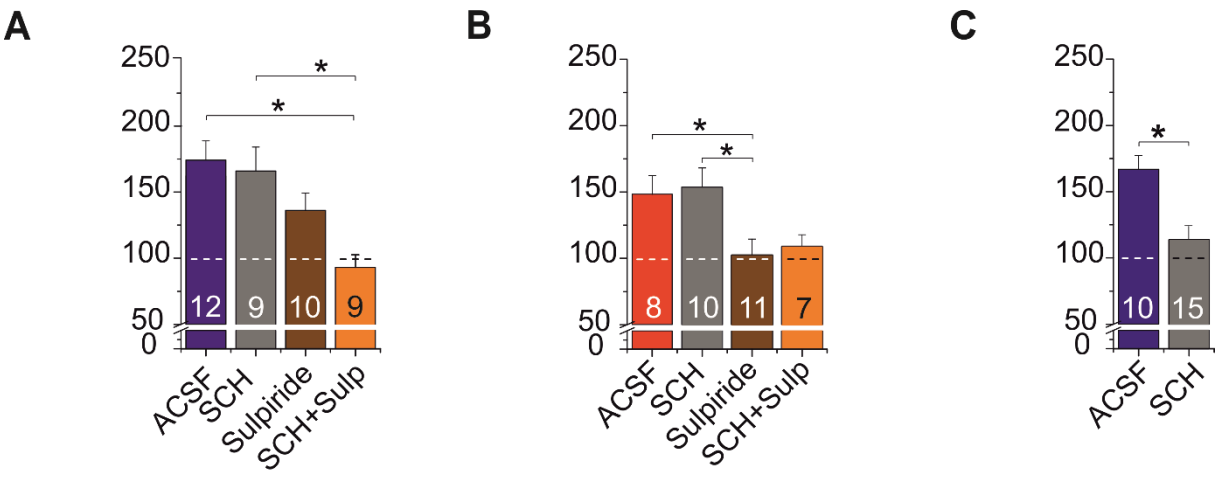

Figure 6: Differential modulation of canonical and burst low repeat t-LTP by dopaminergic signaling. A) *Dependence of 6 x 1:1 t-LTP on D1 and D2 receptor signaling. Neither bath application of SCH23390 (SCH, D1-like antagonist; 10 µM) nor bath application of Sulpiride (Sulp, D2-like antagonist; 10 µM) alone impaired t-LTP (ACSF: n=12 / N=9; SCH23390 n=9 / N=6; Sulpiride n=10 / N=8). However, co-application of both antagonists significantly reduced t-LTP (SCH + Sulp n=9 / N=4).* ***B)*** *T-LTP induced with the 6 x 1:4 protocol was impaired in the presence of Sulpiride, but not further reduced by co-application with SCH23390. Accordingly, application of SCH23390 alone did not affect 6 x 1:4 t-LTP (ACSF: n=8 / N=6; SCH23390 n=10 / N=5; Sulpiride n=11 / N=8; SCH + Sulp n=7 / N=4).* ***C)*** *T-LTP induced with the high repeat (70 x) 1:1 protocol was inhibited in the presence of the D1 receptor antagonist SCH23390 (10 µM) in mouse slices (ACSF n=10 / N=8; SCH23390 n=15 / N=5) to a similar extent as observed previously in rat hippocampal slices (Edelmann and Lessmann, 2011). Mean (± SEM) magnitude of t-LTP is shown for the respective experiments.*

Together, these data indicate that 6 x 1:1 t-LTP depends on D1/D2 receptor co-signaling whereas 6 x 1:4 t-LTP is only dependent on D2 receptors, highlighting a novel and important role of D2 receptors in both types of t-LTP. This is at variance with the fact that most previous studies investigating DA-dependent conventional LTP at SC-CA1 synapses reported an eminent role of D1-like receptors in high frequency induced LTP forms (e.g., Hagena and Manahan-Vaughan, 2016; Papaleonidopoulos et al., 2018). However, our results are fully consistent with the previously described D2 receptor mediated enhancement of t-LTP in the prefrontal cortex (Xu and Yao, 2010), and the prominent role

of D2 receptors in hippocampus-dependent learning (Nyberg et al., 2016). A classical role for D1 receptor signaling was also described for high repeat (70 x) canonical t-LTP in rat hippocampal slices (Edelmann and Lessmann, 2011, 2013). To clarify whether repeat number or species matter for the contribution of D1 and D2 receptors in t-LTP, we examined DA dependence of high repeat 70 x 1:1 t-LTP in mouse hippocampal slices. We found that also in mouse slices 70 x 1:1 t-LTP was fully blocked by bath application of the D1 antagonist SCH23390 (Control: 166.85 ± 11.77, SCH: 113.38 ± 11.07; unpaired Student's t-test, $t_{(22)} = 3.028$; p= 0.0062; **Fig. 6C**). These data reveal that high repeat number induced t-LTP is regulated by D1 signaling whereas D2 signaling is selectively involved in low repeat t-LTP. Further, the extent of D2 receptor involvement in low repeat t-LTP is regulated by the postsynaptic spike pattern used for t-LTP induction (compare **Fig. 6A** and **B**).

The role of BDNF/TrkB signaling in low repeat t-LTP induced by canonical or burst protocols

We recently showed for SC-CA1 synapses that brain-derived neurotrophic factor (BDNF) induced tropomyosin related kinase B (TrkB) signaling mediates t-LTP elicited by a 1:4 t-LTP paradigm with 25 repeats at 0.5 Hz. This t-LTP is driven by an autocrine postsynaptic BDNF/TrkB mechanism that ultimately relies on postsynaptic insertion of new AMPA receptors (Edelmann et al., 2015). To address whether release of endogenous BDNF might be involved also in low repeat t-LTP, we next tested our low repeat t-LTP protocols in slices obtained from heterozygous BDNF knockout ($BDNF^{+/-}$) mice that express ~50% of BDNF protein levels compared to WT littermates (e.g., Endres and Lessmann, 2012; Psotta et al., 2015). Our results show that both types of low repeat t-LTP remained functional in response to this chronic depletion of BDNF (6 x 1:1 t-LTP: WT: 131.37 ± 9.67, BDNF+/-: 134.47 ± 14.85; Mann-Whitney U test, U = 25.0; p = 0.7789; and 6 x 1:4 t-LTP: WT: 134.41 ± 8.78, BDNF+/-: 128.11 ± 8.12; Mann-Whitney U test, U = 14.0; p = 0.5887, **Fig. 7A**). Next, to examine whether acute inhibition of BDNF/TrkB signaling affects low repeat t-LTP, we asked whether scavenging of BDNF by bath applied TrkB receptor bodies (human TrkB-Fc chimera, TrkB-Fc) impairs low repeat canonical or burst t-LTP. However scavenging of BDNF had no effect on the magnitude of t-LTP induced by either of the two protocols (6 x 1:1 t-LTP: ASCF: 157.39 ± 18.19, TrkB-Fc: 173.07 ±

14.05; Mann-Whitney U test, U = 13.0; p = 0.0939 and 6 x 1:4 t-LTP: ACSF: 159.78 ± 10.36, TrkB-Fc: 152.80 ± 20.28; Mann-Whitney U test, U = 22.0; p = 0.8048, **Fig. 7B**).

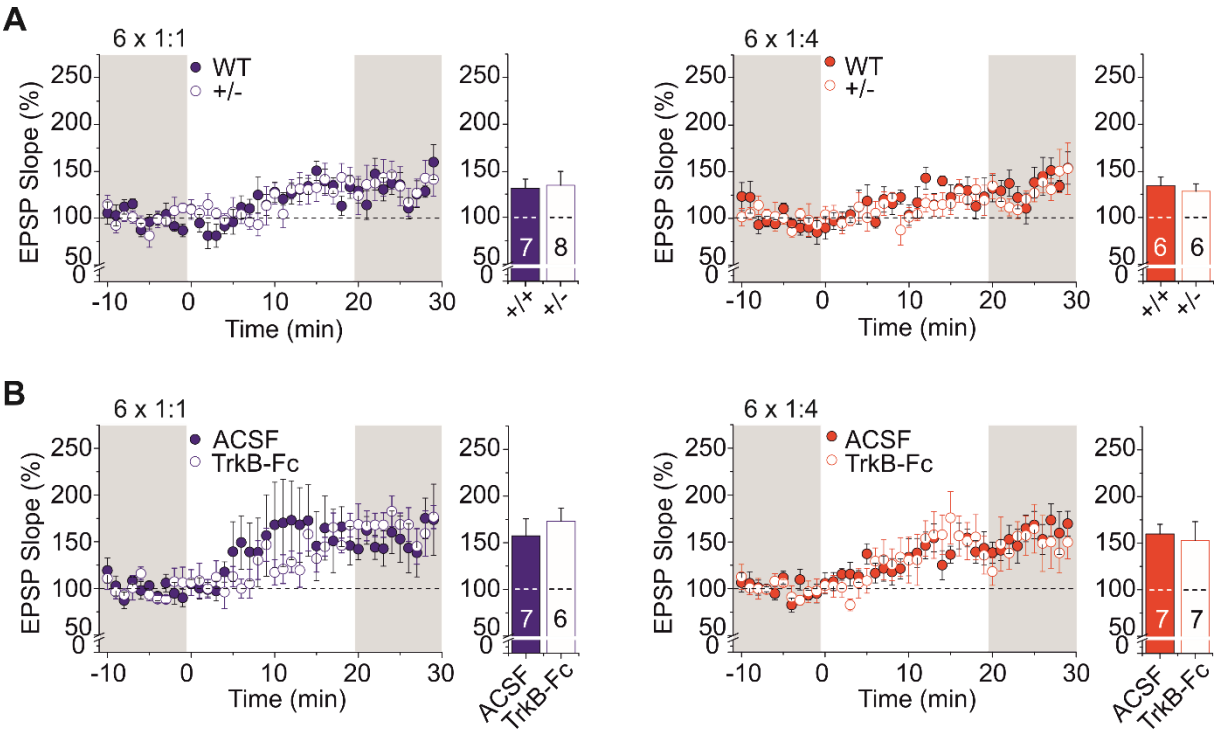

Figure 7: BDNF induced TrkB receptor signaling is not required for t-LTP elicited by low repeat t-LTP protocols. A) *Low repeat t-LTP was not different for 6 x 1:1 (left) and 6 x 1:4 (right) stimulation in heterozygous BDNF knockout animals (+/-) compared to wild type litter mates (+/+) (6 x 1:1: +/+ n =7 / N=6, +/- n=8 / N=7; 6 x 1:4: +/+ n=6 / N=5, +/- n=6 / N=5).* ***B)*** *Bath application of the BDNF scavenger TrkB-Fc (100 ng/ml; 3h preincubation) did not affect t-LTP in response to the two low repeat protocols (left: 6 x 1:1: ACSF n=7 / N=5, TrkB-Fc n=6 / N=6; right: 6 x 1:4: ACSF n=7 / N=5, TrkB-Fc n= 7 / N= 6). Average time course of potentiation and mean (± SEM) magnitude of t-LTP are shown for the respective experiments.*

Together these data indicate that 6 x 1:4 and 6 x 1:1 t-LTP are both independent from activity-dependent release of endogenous BDNF and downstream TrkB signaling. In conjunction with our previous observation that 25 x 1:4 t-LTP is dependent on release of endogenous BDNF (compare Edelmann et al., 2015) the present data suggest that a higher number (>6) of postsynaptic spike bursts in the t-LTP protocol is required to activate BDNF secretion.

467 **The role of GluA2-lacking, calcium-permeable AMPA receptors in low repeat t-LTP**

468 The transient incorporation of GluA2-lacking, Ca^{2+} permeable (cp-) AMPARs after LTP induction has
469 been proposed as an important process to increase postsynaptic Ca^{2+} levels for LTP expression (Kauer
470 and Malenka, 2006; Man, 2011; reviewed in Park et al., 2018; Plant et al., 2006). To examine whether
471 these receptors are involved in low repeat t-LTP, we incubated our recorded hippocampal slices with
472 the selective cp-AMPAR inhibitor NASPM (100 µM). Interestingly, 6 x 1:1 t-LTP and 6 x 1:4 t-LTP were
473 both completely blocked in the presence of NASPM (6 x 1:1: ACSF: 142.81 ± 12.11, NASPM: 89.45 ±
474 9.04; unpaired Student's t-test, $t_{(14)} = 3.3502$; p= 0.0048; 6 x 1:4: ACSF: 177.66 ± 16.83, NASPM:
475 100.32 ± 5.95; unpaired Student's t-test, $t_{(19)} = 4.829$; p= 0.0002, **Fig. 8A, B**). Surprisingly, these
476 results indicate that the influx of Ca^{2+} via GluA2-lacking, cp-AMPARs is mandatory to elicit low-repeat
477 t-LTP induction.
478

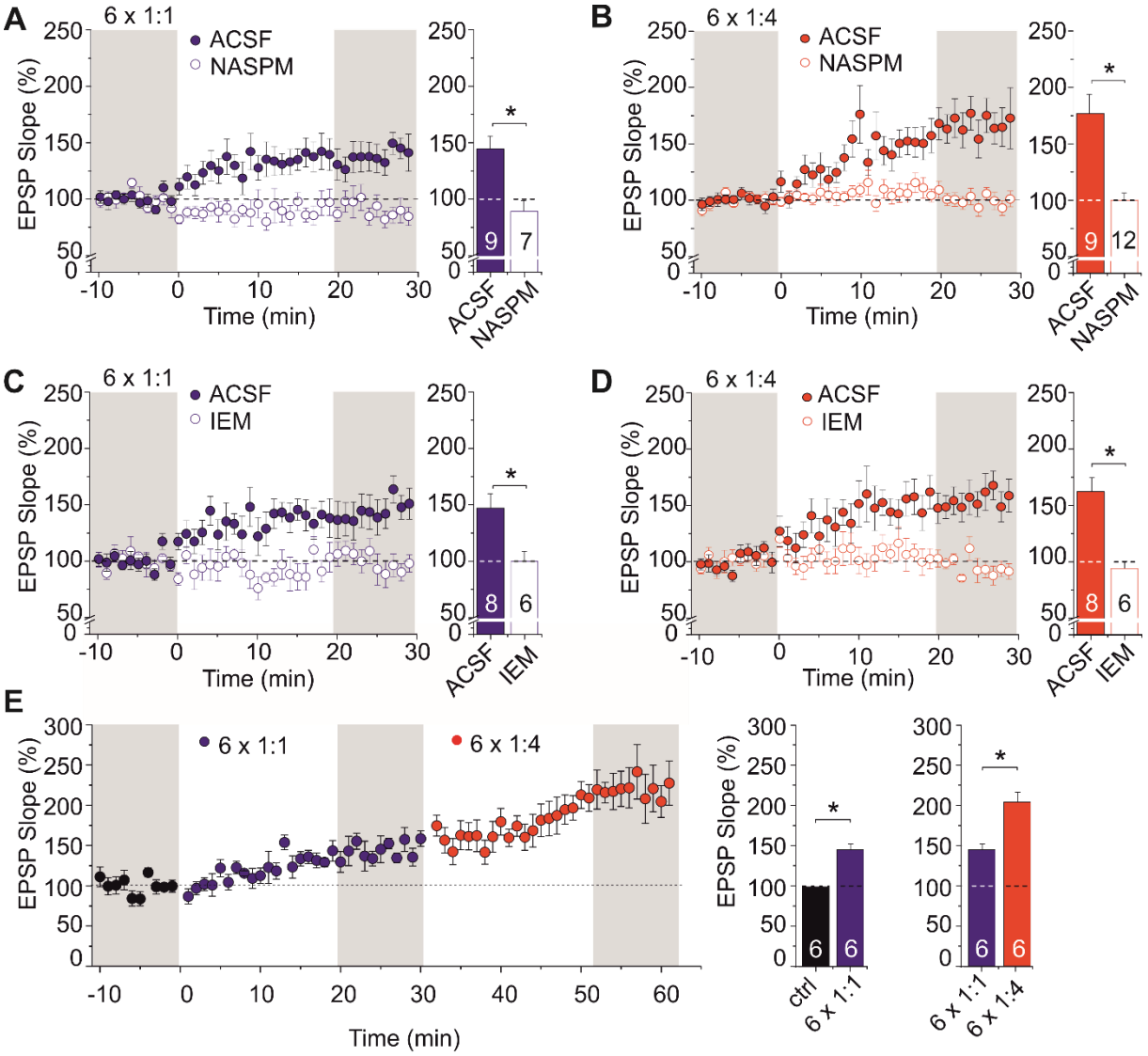

Figure 8: Ca^{2+} influx via GluA2-lacking calcium-permeable AMPARs is required for low-repeat t-LTP induction. *Bath application of a selective inhibitor of Ca^{2+} permeable AMPARs (100 µM NASPM) blocks 6 x 1:1 t-LTP (**A,** 6 x 1:1: ACSF n=9 / N=5, NASPM n=7 / N=3) as well as 6 x 1:4 t-LTP (**B**, 6 x 1:4: ACSF n= 9 / N=6 NASPM n=12 / N=5). Also IEM-1460 (100 µM), a second specific inhibitor of cp-AMPARs, blocks 6 x 1:1 t-LTP (**C,** 6 x 1:1: ACSF n=8 / N=5, IEM-1460 n=6 / N=3) as well as 6 x 1:4 t-LTP (**D**, 6 x 1:4: ACSF n= 8 / N=5, IEM n=6 / N=3). **E**) Successful induction of 6 x 1:1 t-LTP and subsequent 6 x 1:4 t-LTP in the same cells (n=6 / N=3). Note the absence of any signs of occlusion between t-LTP induced by the two low repeat protocols (compare **Fig. S2**). Average time course of potentiation and mean (± SEM) magnitude of t-LTP are shown for the respective experiments*

To rule out off-target effects of NASPM, we verified cp-AMPAR contribution in low repeat t-LTP with a second inhibitor of cp-AMPARs (IEM-1460, 100 µM). As shown in **Figure 8C** and **D**, we observed complete inhibition of low repeat t-LTP also by IEM for both protocols (6 x 1:1: ASCF: 146.99 ±12.56,

493 IEM: 99.89 ± 8.43; unpaired Student's t-test, $t_{(12)}$ = 2.76256; p= 0.0172; 6 x 1:4: ASCF: 162.03 ±12.70,
494 IEM: 94.70 ± 6.24; unpaired Student's t-test, $t_{(12)}$ = 4.4567; p= 0.0007, **Fig. 8C, D**).
495 In light of the many differences in the induction, expression mechanisms, and dopaminergic
496 modulation of the canonical 6 x 1:1 t-LTP and the 6 x 1:4 burst t-LTP we asked whether both types of
497 t-LTP can be elicited completely independent from one another or if they occlude each other. To this
498 aim, we first induced 6 x 1:1 t-LTP followed in the same cells by a subsequently induced 6 x 1:4 t-LTP.
499 As shown in **figure 8C**, both types of t-LTP could be activated independently without any signs of
500 occlusion (1^{st} t-LTP induction (6 x 1:1, 143.68 ± 5.85%): $t_{(5)}$=-3.4618; p= 0.0180; 2^{nd} t-LTP- induction (6
501 x 1:4, 203.17 ± 12.04%): $t_{(5)}$=-4.7081; p= 0.0053, paired Student's t-test). Importantly, in another set
502 of cells, subsequent stimulation for a second time with the same 6 x 1:1 protocol that had already
503 successfully induced t-LTP, did not yield further potentiation (**Fig. S2**; 1^{st} t-LTP induction (6 x 1:1,
504 147.31 ± 13.06%): $t_{(4)}$=-3.4607; p= 0.0258; 2^{nd} t-LTP- induction (6 x 1:1, 157.97 ± 17.88%): $t_{(4)}$=-
505 1.9649; p= 0.1209; paired Student's t-test). Given the strong differences in the induction processes
506 and the presynaptic expression of 6 x 1:1 vs. postsynaptic expression of 6 x 1:4 t-LTP, the absence of
507 occlusion between the two protocols was an expected finding. However, this result highlights the
508 independence of the two different types of low repeat t-LTP investigated here.
509
510 The scheme presented in **figure 9** summarizes our findings for the presynaptically expressed 6 x 1:1 t-
511 LTP and the postsynaptically expressed 6 x 1:4 t-LTP and depicts the putative roles of mGluRs, cp-
512 AMPARs, dopamine signaling, and internal Ca^{2+} stores in low repeat t-LTP. However, since the
513 distribution of dopaminergic fibers and the pre- and/or postsynaptic dopamine receptor localization
514 in the CA1 region is not yet completely clear (compare Edelmann and Lessmann, 2018), further
515 experiments are clearly required to improve the mechanistic understanding of this aspect of low
516 repeat t-LTP. None withstanding, both low repeat t-LTP forms are already by now clearly
517 distinguishable. Their different features of induction and expression mechanisms and the distinct
518 signaling cascades they employ, are likely to form the basis for the versatile computing capacity of
519 individual CA1 neurons in the hippocampus.

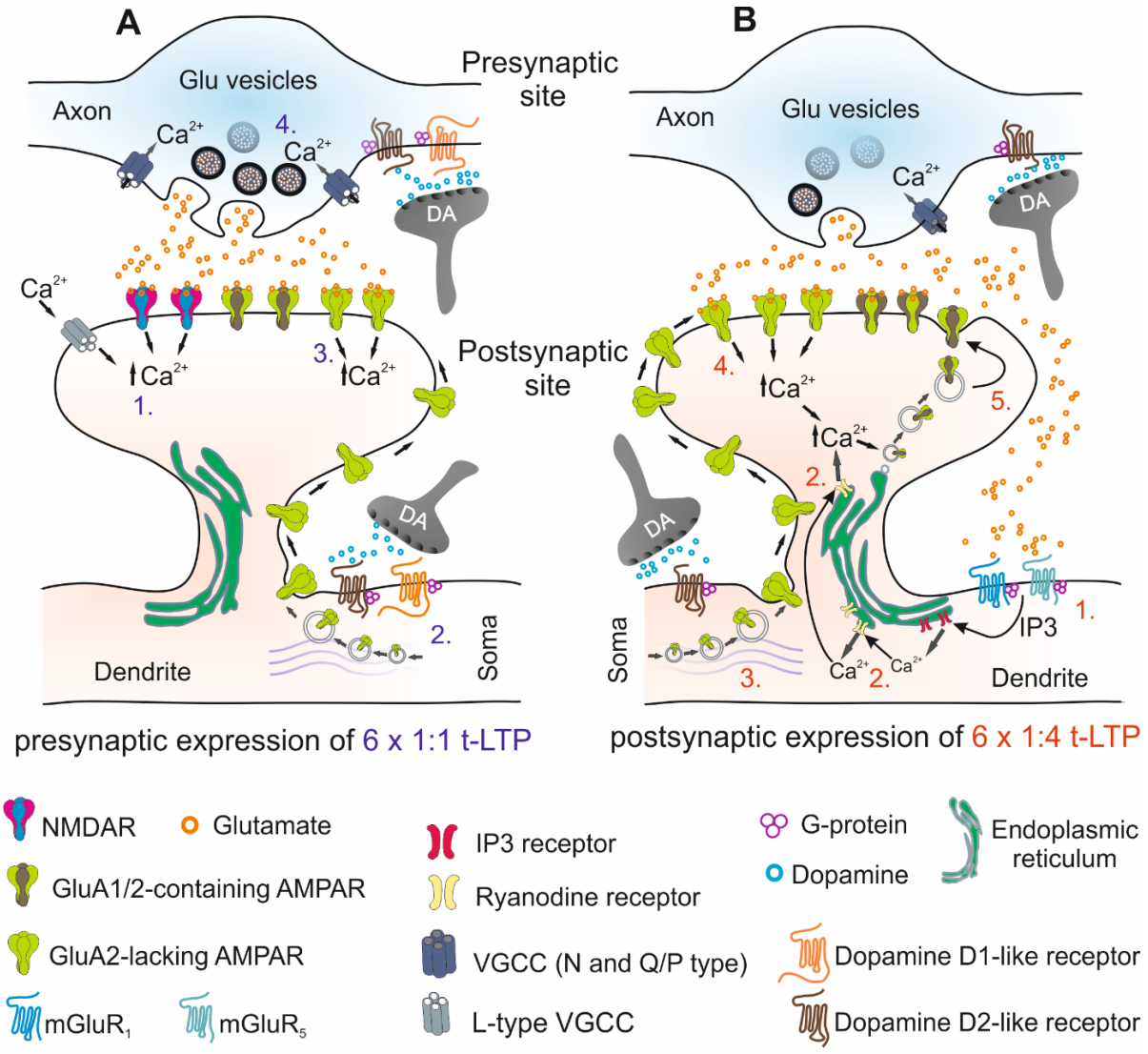

Figure 9: Suggested cellular signaling mechanisms involved in low repeat t-LTP at Schaffer collateral-CA1 synapses. *Summary of induction, signaling, and expression mechanisms involved in low repeat canonical (i.e. 6 x 1:1 t-LTP) and burst (i.e. 6 x 1:4) t-LTP protocols in CA1 pyramidal neurons.* ***A)*** *Synaptic mechanisms involved in the presynaptically expressed 6 x 1:1 t-LTP. T-LTP induction depends on postsynaptic NMDAR and L-type VGCC mediated Ca^{2+} influx (1.). Insertion of cp-AMPARs into the postsynaptic membrane might be regulated by D1/D2 signaling (2.) and could account for the combined D1/D2 receptor dependence of 6 x 1:1 t-LTP. Ongoing low frequency test stimulation after induction of t-LTP leads to sustained Ca^{2+} elevations through postsynaptic cp-AMPARs (3.). The resulting prolonged postsynaptic Ca^{2+} elevation leads via a yet unidentified retrograde messenger to increased presynaptic efficacy (4.). An additional presynaptic contribution of D1/D2 signaling to enhanced presynaptic glutamatergic function is possible.* ***B)*** *The postsynaptically expressed 6 x 1:4 t-LTP does neither require postsynaptic NMDAR nor L-type VGCC activation for induction. It rather depends on calcium release from postsynaptic internal stores mediated by*

535 *mGluR$_{1,5}$-dependent activation of IP3 receptors in the ER (1.). This initial postsynaptic Ca^{2+} rise is*
536 *amplified by Ca^{2+} dependent Ca^{2+} release via Ryanodine receptors (RyRs; 2.). Moreover, the 6 x 1:4 t-*
537 *LTP depends (like 6 x 1:1 t-LTP) on the activation of cp-AMPARs. Intact D2 receptor signaling is*
538 *mandatory to observe 6 x 1:4 t-LTP and might be involved in recruiting cp-AMPARs to the*
539 *postsynaptic membrane (3.) for sustained Ca^{2+} influx during ongoing low frequency synaptic*
540 *stimulation after t-LTP induction (4.). The resulting prolonged postsynaptic Ca^{2+} elevation initiated by*
541 *mGluRs, RyRs, and cp-AMPARs leads to postsynaptic expression of 6 x 1:4 t-LTP by insertion of new*
542 *GluA1 and GluA2-containing AMPARs into the postsynaptic membrane (5.)*
543
544
545

Discussion

Our study shows that t-LTP at hippocampal SC-CA1 synapses requires only six repeats of coincident presynaptic stimulation paired with either 1 or 4 postsynaptic spikes at low frequency (0.5 Hz). For the 1:4 burst protocol, even just three repeats are sufficient to elicit t-LTP. The 6 x 1:1 t-LTP was induced by Ca^{2+} influx via postsynaptic NMDARs and L-type VGCCs, occurred independent of BDNF release, and required combined D1/D2 receptor signaling. In contrast, the 6 x 1:4 t-LTP was induced by postsynaptic Ca^{2+} release from internal stores mediated via mGluRs/IP_3 signaling and ryanodine receptors, and was completely inhibited in the presence of D2 receptor antagonists. Both, low repeat canonical and burst t-LTP, strongly depended on activation of GluA2-lacking cp-AMPARs. These data suggest that low repeat STDP paradigms with potentially high physiological relevance can induce equally robust t-LTP as observed for high repeat t-LTP in the hippocampus. However, the pharmacological profile of low repeat t-LTP induction and expression revealed astonishingly subtle differences between both induction protocols.

Dependence of t-LTP on repeat number and frequency of the STDP stimulation

Both 6 x t-LTP protocols used in our study yielded robust t-LTP with similar time courses as described previously for standard STDP paradigms that used either higher number of pairings or higher pairing frequency (compare e.g., Carlisle et al., 2008; Couey et al., 2007; Edelmann et al., 2015; Seol et al., 2007; Tigaret et al., 2016; Wittenberg and Wang, 2006; Yang and Dani, 2014). To date, only few studies focused on STDP protocols with low numbers of repeats for t-LTP induction (Cui et al., 2016; discussed in Edelmann et al., 2017; Froemke et al., 2006; Zhang et al., 2009). Since only such low repeat t-LTP protocols can be completed within a few seconds, these protocols are likely to represent a very physiological model for synaptic plasticity events triggering learning and memory processes that can also occur on a timescale of seconds. Thus, investigating the underlying signaling mechanisms appears to be relevant for learning induced synaptic changes *in vivo*. Similar to the results of Froemke and colleagues (Froemke et al., 2006) for layer 2/3 cortical neurons, we observed

no significant difference in the magnitude of 1:1 t-LTP between the threshold repeat number (i.e., 6 repeats at 0.5 Hz) and higher repeat numbers at hippocampal Schaffer collateral (SC)–CA1 synapses (25 and 70 repeats; compare **Fig. 1A**). As for the canonical protocol, we also determined the threshold for successful t-LTP induction also for the burst protocol (compare **Fig. 1B**). The observed shift of the threshold repeat number to lower values (3 instead of 6 repeats for successful 1:4 t-LTP induction) for the burst protocol speaks in favor of facilitated postsynaptic induction by the spike train instead of single spikes used by the 1:1 protocol (compare Remy and Spruston, 2007). Although 35 repeats of the burst protocol showed a tendency towards reduced magnitude of t-LTP, the efficacy of 3, 6 and 35 repeats of 1:4 t-LTP were not significantly different. Together these data suggest that depending on the exact pattern (e.g., 1:1 vs. 1:4 paradigm) used for t-LTP induction distinct thresholds for the successful number of repeats can be observed.

Bittner and colleagues recently described in elegant *in vivo* recordings synaptic plasticity in mouse hippocampal place cells that can be triggered by pairing low numbers of postsynaptic action potentials with long-lasting dendritic depolarization, which works equally well with positive and negative pairing delays of roughly 1 s (Bittner et al., 2015; Bittner et al., 2017). While their work provides compelling evidence for the physiological relevance of low repeat spiking induced LTP for learning, this behavioral time scale synaptic plasticity follows a non-hebbian mechanism. In contrast, our low repeat t-LTP follows hebbian rules, since only simultaneous and nearly coincident pre- and postsynaptic pairing with positive timing delays leads to associative potentiation (compare **Fig. 2C**). Nevertheless, also such hebbian t-LTP protocols have been described previously to allow extension of STDP to behavioral time scales (compare e.g., Drew and Abbott, 2006; Gerstner et al., 2018; Shindou et al., 2019). In case of our low repeat t-LTP protocols, with the six repeat protocol comprising overall 10 s, and the three repeat protocol occurring within overall 4 s, this duration might bridge the time window between millisecond-dependent STDP and learned behavior on the time scale of several seconds.

In cultured hippocampal neurons, Zhang and colleagues (Zhang et al., 2009) showed that more than 10 repeats of their 1:1 STDP protocol were necessary to induce t-LTP. However, bath application of dopamine facilitated t-LTP induction and reduced the number of pairings that were required at a given frequency to successfully induce t-LTP (Zhang et al., 2009). Since primary cultures of dissociated hippocampal neurons develop synaptic connections in the absence of dopaminergic inputs, the role of endogenous DA can be investigated only if t-LTP is recorded in acutely isolated hippocampal slices as performed here. Interestingly, our data show that both low repeat t-LTP variants tested are blocked when signaling of endogenously released DA is inhibited (**Fig. 6**). Our results are in line with the previously described effects of exogenously added DA on t-LTP in hippocampal cultures (Zhang et al., 2009). The release of endogenous DA in our slices (Edelmann and Lessmann, 2011, 2013) is therefore likely to account for the low number of repeats required for successful induction of t-LTP in our study. Whether this effect is due to acute release of DA from axon terminals elicited via the extracellular co-stimulation of dopaminergic afferents during t-LTP induction and test stimulation or rather depends on ambient levels of DA in the slices remains to be determined.

Regarding the magnitude of t-LTP induced by low repeat canonical and burst protocols we, found that both, 6 x 1:1 and 6 x 1:4 t-LTP, were equally successful to induce t-LTP at positive spike timings (**Fig. 2C**). Because it is reasonable to assume that 1:4 burst protocols induce longer lasting and stronger Ca^{2+} elevations than 1:1 pairings, it might be expected that the time course of synaptic potentiation could differ between the two protocols. However, both protocols induced t-LTP with comparable onsets and rise times of potentiation and also resulted in similar magnitudes of t-LTP after 1 h of recording (compare **Fig. 2D**). Thus, except for the lower threshold number of repeats to elicit t-LTP (see last paragraph), the burst protocol does not seem to be more effective in inducing t-LTP at SC-CA1 synapses than the canonical protocol.

We also compared different spike timings (with negative and positive delays), to compare the full capacity to induce bidirectional plasticity with low repeat protocols (**Fig. 2A, B**). For positive pairings with Δt: +20 ms we observed a similar decline (compared to Δt: +10 ms) in t-LTP magnitude as

626 described previously for higher numbers of repeats (compare Bi and Poo, 1998; Edelmann et al.,
627 2015). When applying negative pairings (i.e. post before pre pairings) t-LTP was absent, but we did
628 not observe robust t-LTD for either of the two protocols. While these results stress that successful
629 induction of t-LTP is critically dependent on the sequence of presynaptic and postsynaptic spiking
630 and on the pairing interval, future studies should address under which conditions low repeat t-LTD
631 can be induced by anti-causal synaptic activation.
632
633 **Mechanisms of expression of low repeat t-LTP**
634 Despite the similarities described above, both low repeat protocols recruited different expression
635 mechanisms. Synaptic potentiation induced with the 6 x 1:1 protocol is most likely expressed by
636 presynaptic alterations (see below), whereas the 6 x 1:4 protocol relies on postsynaptic insertion of
637 AMPA receptors (**Fig. 3**). Commonly, LTP at SC-CA1 synapses that is induced by high-frequency
638 stimulation and is also thought to be expressed by a postsynaptic increase in AMPA receptor
639 mediated currents (Granger and Nicoll, 2014; Nicoll, 2003). For STDP, however, different mechanisms
640 of expression have been described that varied between brain regions and depending on
641 experimental conditions (see e.g., Costa et al., 2017). Even at a given type of synapse (i.e.
642 hippocampal SC-CA1) t-LTP can be expressed either pre- or postsynaptically (Edelmann et al., 2015).
643 At this synapse, the expression mechanism of LTP seemed to be encoded by the pairing pattern used
644 for STDP. While t-LTP induced by 70 x 1:1 stimulation was expressed via increased presynaptic
645 glutamate release, a 35 x 1:4 t-LTP was expressed via insertion of additional AMPARs by a GluA1-
646 dependent mechanism (Edelmann et al., 2015). However, in this previous study, we used different
647 numbers of repeats for the two t-LTP protocols (i.e. 20-35 x 1:4 and 70-100 x 1:1) to keep
648 postsynaptic activity at an equivalent level. Those previous results did not allow to distinguish
649 whether repeat number or stimulation pattern determined the site of t-LTP expression. With help of
650 our current experiments using fixed numbers of repeats for both protocols, we could now determine
651 that the pattern of postsynaptic spiking and not the repeat number influences the expression locus
652 for t-LTP (compare **Fig. 3**).

For the 6 x 1:1 t-LTP, the absence of an increase in AMPAR mediated currents (**Fig. 5**) and the observed decrease in paired pulse ratio (PPR) after successful LTP induction and the increased mEPSC frequency (**Fig. S1**), are consistent with presynaptic enhancement of glutamate release probability. Regarding the retrograde messenger required for both types of 1:1 t-LTP our data indicate that neither NO nor endocannabinoids are involved in the presynaptic expression (data not shown). However, further investigating the underlying presynaptic mechanisms of 6 x 1:1 t-LTP was beyond the scope of the current study. The six repeat version of our burst t-LTP protocol (6 x 1:4) seems to follow the suggested mechanisms for conventional SC-CA1 LTP, with postsynaptic expression via insertion of new AMPARs leading to increased AMPAR mediated currents and the absence of significant changes in paired pulse facilitation, as previously also described for high repeat burst t-LTP (Edelmann et al., 2015). Furthermore, our experiments with Pep1-TGL clearly demonstrate the importance of GluA1 containing AMPARs for the expression of 6 x 1:4 t-LTP (**Fig. 3C**).

Dependence of low repeat t-LTP induction on different sources for postsynaptic Ca^{2+} elevation

Induction of t-LTP with low repeat STDP protocols as a model to investigate physiologically relevant synaptic plasticity mechanisms has just started. Accordingly, the contribution of different sources of Ca^{2+} to its induction was until now largely unknown. Unexpectedly, our experiments revealed distinctly different routes for postsynaptic Ca^{2+} elevation for the low repeat 1:1 and 1:4 protocol to induce t-LTP. The results for the 6 x 1:1 t-LTP are in accordance with previous studies showing that t-LTP as well as classical high frequency stimulation induced LTP at CA1 glutamatergic synapses rely on Ca^{2+} influx via postsynaptic NMDA receptors (Malenka and Bear, 2004). For STDP, NMDARs are thought to serve as coincidence detectors of timed pre- and postsynaptic activation (e.g., Bi and Poo, 1998; Debanne et al., 1998; Edelmann et al., 2015; Feldman, 2000). Depending on the level of postsynaptic Ca^{2+} that is reached during induction, separate signaling cascades leading to either LTP or LTD are activated (Artola and Singer, 1993; cited in Caporale and Dan, 2008; Lisman, 1989). For t-LTD, alternative mechanisms for coincidence detection have been described (Bender et al., 2006;

Fino and Venance, 2010). Instead of NMDAR-mediated Ca^{2+} influx, these studies reported that either mGluRs, L-type VGCCs or IP3 gated internal Ca^{2+} stores can trigger the induction of LTD. As for LTD, also for LTP, additional coincidence detectors and Ca^{2+} sources might be involved in its induction (Dudman et al., 2007; VGCC: Magee and Johnston, 1997; Nanou et al., 2016; IP3-sensitive stores: Takechi et al., 1998; Wang et al., 2016; Wiera et al., 2017). In accordance with these previous studies, we found that 6 x 1:1 t-LTP can in addition to NMDARs also be induced by Ca^{2+} entry through L-type VGCCs (**Fig. 4A, C**).

In contrast to these conventional Ca^{2+} sources for the canonical low repeat t-LTP, the situation is much different for 6 x 1:4 burst t-LTP. Although a requirement for postsynaptic Ca^{2+} elevation is clearly evident from the BAPTA experiments (**Fig. 5A**), Ca^{2+} entry via NMDARs or L-type VGCCs was not involved (compare **Fig. 4B, D**). Rather, our results demonstrated that the initial postsynaptic Ca^{2+} rise involved group I mGluRs (i.e. $mGluR_1$ and $mGluR_5$; Kaar and Rae, 2015), subsequent activation of IP_3Rs and RyRs, eventually activating GluA2-lacking Ca^{2+}-permeable AMPARs in the postsynaptic membrane (compare **Figs. 5** and **8**). While activation of mGluRs seems to contribute to the initial postsynaptic Ca^{2+} rise in 6 x 1:4 t-LTP, subsequent Ca^{2+} induced Ca^{2+} release via RyRs amplifies and prolongs this Ca^{2+} signal (compare **Fig. 5D**). The initial rise in postsynaptic Ca^{2+} levels might be co-induced by Ca^{2+} influx through GluA2 subunit deficient Ca^{2+}-permeable AMPA receptors (cp-AMPARs) into the postsynaptic cell (Suzuki et al., 2001) . This is evident from our experiments performed in the presence of the mGluR antagonists, IP_3R inhibitors and the antagonists of Ca^{2+} permeable AMPARs NASPM and IEM, which completely inhibited 6 x 1:4 t-LTP (group I mGluR: **Fig. 5B**, C, cp-AMPAR: **Fig. 8B, D**, for discussion of cp-AMPAR, see below).

Group I metabotropic GluR have indeed been described previously to contribute to certain types of hippocampal LTP (Wang et al., 2016), while our present results show for the first time their involvement in STDP. Altogether it seems plausible that 6 x 1:4 stimulation first activates $mGluR_{1,5}$ receptors, which subsequently trigger IP_3- mediated calcium release from internal stores (Jong et al., 2014, compare **Fig. 5D**). The resulting calcium rise and additional Ca^{2+} influx via cp-AMPARs might

706 than be strengthened by additional IP_3 and RyR mediated calcium induced Ca^{2+} release to
707 successfully boost low repeat induced burst t-LTP (compare **Fig. 9**).
708
709 **Regulation of low repeat t-LTP by dopamine receptor signaling**
710 The accurate timing of pre- and postsynaptic activity is necessary for hebbian plasticity. In addition,
711 neuromodulator signaling critically regulates the efficacy of STDP protocols to elicit t-LTP (e.g.,
712 Cassenaer and Laurent, 2012; Cui et al., 2015; Edelmann et al., 2015; Edelmann et al., 2017;
713 Edelmann and Lessmann, 2011, 2018; Pawlak and Kerr, 2008; Seol et al., 2007; Yang and Dani, 2014;
714 Zhang et al., 2009). Since high repeat STDP in the hippocampus is regulated by dopamine (DA, e.g.,
715 Edelmann and Lessmann, 2013), we also investigated DAergic modulation of our two low repeat
716 STDP variants (compare **Fig. 6**). While both low repeat t-LTP protocols were dependent on
717 endogenous DA signaling, the pharmacological profile for them was quite different. The 6 x 1:4 t-LTP
718 was completely dependent on intact D2 receptor signaling, but independent from D1 receptor
719 activation. This result can be easily reconciled with pure D2 receptor dependent signaling being
720 responsible for induction of the 6 x 1:4 t-LTP (compare **Fig. 6B**). Little is known about D2R mediated
721 function in t-LTP as well as in classical LTP. It was shown, however, that D2 receptors can limit
722 feedforward inhibition in the prefrontal cortex and allow thereby more effective t-LTP (Xu and Yao,
723 2010). Importantly, D2 like receptors are expressed in the hippocampus in pre- and postsynaptic
724 neurons and have been described to regulate synaptic plasticity (Beaulieu and Gainetdinov, 2011;
725 Dubovyk and Manahan-Vaughan, 2019; Sokoloff et al., 2006). Moreover, D2 receptors contribute to
726 hippocampus-dependent cognitive functions (Nyberg et al., 2016). Together, these previous results
727 on D2 receptor mediated functions in the hippocampus are clearly in line with the role in 6 x 1:4 t-
728 LTP in our experiments. In contrast to the 6 repeat burst protocol, the 6 x 1:1 t-LTP remained
729 functional when either D1-like or D2-like dopamine receptor signaling was intact. Although inhibition
730 of D2 receptors by Sulpiride had a tendency to reduce the magnitude of the 1:1 t-LTP, this effect did
731 not reach statistical significance. Moreover, while the D1 receptor inhibitor SCH23390 alone did not
732 show any signs of 6 x 1:1 t-LTP inhibition, it was nevertheless able to impair the slightly reduced t-LTP

733 in the presence of Sulpiride down to control levels, when both antagonists were co-applied (**Fig. 6A**).
734 The interpretation of this pharmacological profile of 6 x 1:1 t-LTP needs to take into consideration
735 that D1-like and D2-like receptors do not signal exclusively via altering cAMP levels (cAMP increase
736 via D1-like receptors - or decreased via D2-like receptors; Tritsch and Sabatini, 2012). Rather, D5
737 receptors and heterodimeric D1/D2 receptors can also activate cAMP-independent PLC pathways
738 stimulating in turn IP_3/Ca^{2+}, DAG/PKC signaling, or MAPK signaling downstream of D1 receptor
739 activation and Akt kinase signaling. Also direct modulation of NMDARs and VGCCs in response to D2R
740 activation is possible (Beaulieu and Gainetdinov, 2011). Consequently, the question whether the
741 combined D1 -like/D2 -like receptor dependence of the 1:1 t-LTP reflects rather the activation of
742 D1/D2 heteromeric receptors, or distinct pre- vs. postsynaptic expression and signaling of D1 and D2
743 receptors at SC-CA1 synapses needs to be addressed by future experiments.
744 To interpret the combined regulation of the 6 x 1:1 t-LTP by D1- and D2-like receptors it also needs to
745 be taken into consideration that D2-like receptors are generally believed to display a higher affinity
746 for DA compared to D1-like receptors (Beaulieu and Gainetdinov, 2011). Therefore, the complex D1-
747 and D2 receptor-dependent regulation of 6 x 1:1 t-LTP might assure that this type of t-LTP is on the
748 one hand regulated by the presence of DA, but on the other hand remains intact at high and low DA
749 concentrations. On the same vein, this co-regulation could assure that slowly rising ambient DA
750 levels created by tonic firing of DAergic neurons are equally effective in regulating 6 x 1:1 t-LTP as
751 much faster rising DA concentrations during phasic firing.
752 Such a change in DA release was indeed shown in recordings of midbrain neurons, where activity of
753 DAergic neurons switches from tonic to phasic burst activity resulting in locally distinct levels of
754 secreted DA in the target regions (Rosen et al., 2015). Local DA concentration differences can then
755 result in different DA-dependent effects, with high affinity D2-like receptors being activated by low
756 and slowly rising extracellular DA levels, while low affinity D1 receptors are only activated by local DA
757 peaks.
758 For our STDP experiments where DAergic input fibers are most likely co-activated during SC
759 stimulation, we observed similar activity-dependent recruitment of different DA receptors. While D1

760 receptor-dependent effects were activated by 70-100 stimulations (Edelmann and Lessmann, 2011
761 and compare **Fig. 6C**), D1/D2 receptors or pure D2 receptor mediated processes were already
762 activated by six presynaptic co-stimulations of DAergic fibers (compare **Fig. 6A, B**). Taking into
763 account that D2-like receptors (i.e. D2, D3 and D4 receptors) are classically thought to inhibit LTP by
764 decreasing cAMP/PKA signaling (Otmakhov and Lisman, 2002; Otmakhova et al., 2000), D2-like
765 receptor driven t-LTP processes might indeed be activated by $G_{\beta\gamma}$ signaling independent of cAMP
766 pathways. As mentioned above, $G_{\beta\gamma}$ signaling also blocks L-type and N-type VGCCs (Tritsch and
767 Sabatini, 2012) and D2 receptor signaling can yield Ca^{2+} release from internal stores - two
768 mechanisms that might account for the uncommon type of calcium source required for the induction
769 of our 6 x 1:4 t-LTP (compare **Figs. 4 and 5**).
770
771 **Independence of low repeat t-LTP on BDNF/TrkB signaling**
772 Brain-derived neurotrophic factor (BDNF) is well known for its important role in mediating long-
773 lasting changes of synaptic plasticity (reviewed in e.g., Edelmann et al., 2014; Gottmann et al., 2009;
774 Lessmann et al., 2003; Park and Poo, 2013). Moreover, BDNF is also involved in regulating STDP
775 (Edelmann et al., 2015; Lu et al., 2014; Sivakumaran et al., 2009). For hippocampal SC-CA1 synapses it
776 was shown that BDNF is secreted from postsynaptic CA1 neurons in response to 20-35 repeats of a
777 1:4 STDP protocol mediating postsynaptically expressed t-LTP via postsynaptic TrkB receptor
778 activation (Edelmann et al., 2015). Interestingly, the results of the present study revealed, that
779 neither of the two low repeat t-LTP variants depended on BDNF induced TrkB signaling (compare **Fig.**
780 **7**). This finding was not unexpected since release of endogenous BDNF has been reported previously
781 to require more prolonged barrages of AP firing than just 6 repeats of short AP (burst) firing at 0.5 Hz
782 (compare Balkowiec and Katz, 2002; Edelmann et al., 2015; Lu et al., 2014; Brigadski et al., 2019).
783 This BDNF independency was observed in situations with either chronic (e.g., heterozygous BDNF
784 knockout animals) or acute depletion of BDNF (BDNF scavenger; see e.g., Edelmann et al., 2015; Meis
785 et al., 2012; Schildt et al., 2013).
786

Function of GluA2-lacking Ca^{2+} permeable AMPA receptors in low repeat t-LTP

Interestingly, both variants of low repeat t-LTP were strictly dependent on activation of GluA2-lacking calcium-permeable (cp-)AMPA receptors (**Fig. 8**). In the respective experiments, NASPM or IEM were present in the ACSF from the start of the recording to assure complete inhibition of cp-AMPARs during t-LTP induction. The respective solvent controls were treated in the same way. In CA1 neurons, cp-AMPARs were described to be absent from postsynaptic membranes during basal synaptic stimulation. Rather, they were reported to transiently insert into the postsynaptic membrane after tetanic LTP stimulation to allow sustained Ca^{2+} influx into the postsynaptic neuron after LTP induction, thereby facilitating expression of late LTP (reviewed in Park et al., 2018). A role of cp-AMPARs in STDP has thus far not been reported and these results represent a crucial new finding that emerges from our study. Additional experiments will be required to determine the time course of activity-dependent cp-AMPAR incorporation during induction of low repeat t-LTP into the postsynaptic membrane. Furthermore, it needs to be determined how cp-AMPAR mediated Ca^{2+} influx is orchestrated with mGluR- and RyR-dependent Ca^{2+} elevation for induction of low repeat 6 x 1:4 t-LTP. Likewise, the co-operation of cp-AMPARs with NMDAR- and VGCC-dependent Ca^{2+} elevations for inducing 6 x 1:1 t-LTP needs to be investigated.

In addition to allowing sufficient Ca^{2+} elevation in t-LTP, cp-AMPARs might be involved in DA-dependent priming of synapses for delayed/retroactive reinforcement of LTP or silent eligibility traces (e.g., Brzosko et al., 2015; Gerstner et al., 2018; He et al., 2015; Shindou et al., 2019). By those eligibility traces or delayed reinforcements, the different time scales between milliseconds and seconds can be bridged, to connect hebbian synaptic plasticity to behavioral responses and learning. Such mechanisms might also be involved in the signaling mechanisms employed by our low repeat t-LTP protocols (6 x 1:1 and 6 x 1:4), since both variants of t-LTP show a clear dependence on DA signaling and on cp-AMPARs (compare **Figs 6** and **8**).

In summary, we used two different low repeat STDP protocols at SC-CA1 synapses to record synaptic plasticity at the single cell level in postsynaptic CA1 neurons (i.e. t-LTP). We found that, dependent

on stimulation pattern and repeat number, distinct signaling and expression mechanisms are activated by the canonical and the burst low repeat paradigm. From our experiments, we can conclude that even with the same experimental setup, age and species, multiple types of synaptic plasticity mechanisms can coexist at a given type of synapse. This plethora of coexisting plasticity mechanisms for strengthening synaptic transmission seems to be ideally suited to empower the hippocampus to fulfill its multiplexed functions in memory storage.

Material and Methods

Preparation of hippocampal slices

Horizontal hippocampal slices (350 µm thickness) were prepared from 4 weeks old male wild type C57BL/6J (Charles River), $BDNF^{+/-}$ or littermate control mice (Korte et al., 1995; all animals bred on a C57BL/6J background), according to the ethical guidelines for the use of animal in experiments, and were carried out in accordance with the European Committee Council Directive (2010/63/EU) and approved by the local animal care committee (Landesverwaltungsamt Sachsen-Anhalt).

Briefly, mice were decapitated under deep anesthesia with forene (Isofluran CP, cp-pharma, Germany) and the brain was rapidly dissected and transferred into ice-cold artificial cerebrospinal fluid (ACSF) cutting solution (125 mM NaCl, 2.5 mM KCl, 0.8 mM NaH_2PO_4, 25 mM $NaHCO_3$, 25 mM Glucose, 6 mM $MgCl_2$, 1 mM $CaCl_2$; pH 7.4; 300-303 mOsmol/kg), saturated with 95% O_2 and 5% CO_2. Blocks from both hemispheres containing the hippocampus and the entorhinal cortex were sectioned with a vibratome (VT 1200 S, Leica, Germany). Slices were incubated for 35 min at 32°C in a handmade interface chamber containing carboxygenated ACSF cutting solution and then transferred to room temperature (~21°C) for at least 1 hour before the recording started. Whole cell patch-clamp recordings were performed in submerged slices in a recording chamber with continuous perfusion (1-2 ml per min) of pre-warmed (30 ± 0.2°C) carboxygenated physiological ACSF solution (125 mM NaCl, 2.5 mM KCl, 0.8 mM NaH_2PO_4, 25 mM $NaHCO_3$, 25 mM Glucose, 1 mM $MgCl_2$, 2 mM $CaCl_2$; pH 7.4; 300-303 mOsmol/kg). For all experiments, 100 µM Picrotoxin ($GABA_A$ blocker) was added to ACSF

841 solution. Epileptiform activity by activation of recurrent CA3 synapses was prevented by a cut
842 between CA3 and CA1 subfields (compare Edelmann et al., 2015). To reduce the amount of inhibitors
843 in some of the experiments (e.g. application of NASPM and IEM-1460) we used a micro-perfusion
844 pump-driven solution recycling system (Bioptechs Delta T Micro-Perfusion pump high flow,
845 ChromaPhor, Germany) to limit the volume of solution for incubation of slices (Meis et al., 2012).
846 Both, NASPM and IEM were applied 15 min prior to STDP induction. The drugs were present during
847 the whole experiment. Respective matched control experiments were performed under identical
848 conditions to assure that the microperfusion recycling of ACSF alone did not affect t-LTP.
849
850 **Electrophysiological recordings**
851 Whole cell patch-clamp recordings were performed on pyramidal neurons in the CA1 subregion of
852 the intermediate hippocampus under visual control with infrared DIC-videomicroscopy (RT-SE series;
853 Diagnostic instruments, Michigan, USA). The pipettes (resistance 5-7 MΩ) were filled with internal
854 solution containing (in mM): 10 HEPES, 20 KCl, 115 potassium gluconate, 0-0.00075 $CaCl_2$, 10 Na
855 phosphocreatine, 0.3 Na-GTP, and 4 Mg-ATP (pH 7.4, 285-290 mOsmol/kg). Cells were held at -70 mV
856 in current clamp or voltage clamp (liquid junction potential of +10 mV of internal solution was
857 corrected manually) with an EPC-8 patch clamp amplifier (HEKA, Lamprecht, Germany). Extracellular
858 stimulation of the Schaffer collateral (SC) fibers to generate an excitatory postsynaptic potential
859 (EPSP, at 0.05Hz) was induced either by glass stimulation electrodes (resistance 0.7 – 0.9 MΩ) or a
860 concentric bipolar electrode (FHC; Bowdoin, USA) positioned in Stratum radiatum (SR) of the CA1
861 subregion. The stimulus intensity was adjusted to evoke responses with amplitudes of 4-5 mV
862 corresponding to 30-50% of maximal EPSP amplitudes. Stimulus duration was set to 0.7 ms with
863 intensities ranging between 90 to 700 µA.
864
865 **Induction of Spike timing-dependent plasticity**
866 Spike timing-dependent plasticity (STDP) was induced by pairing of an individual EPSP, generated by
867 extracellular stimulation of SC, with a single action potential (AP) or with a burst of 4 APs (frequency

200 Hz) induced by somatic current injection (2 ms; 1 nA) through the recording electrode (Edelmann et al., 2015). Pairings of postsynaptic EPSP and APs were usually performed with a time interval of +10 ms, and were repeated 2-70 times at a frequency of 0.5 Hz to elicit t-LTP. In some experiments, either longer time windows (positive spike timings: Δt= +17-25 ms, binned as 20 ms data) were used to test t-LTP at longer Δt or short negative spike timings (Δt= -15ms) were used to test effects of anti-causal synaptic stimulation. EPSPs were monitored every 20 s (i.e., 0.05 Hz) for 10 min baseline and then 30 min or 60 min after STDP induction. Unpaired stimulation of 4 postsynaptic APs instead of a full STDP protocol were performed (i.e., 6x 0:4) in a subset of cells that served as controls. In another set of cells, we assessed possible spontaneous changes in synaptic transmission (stimulation at 0.05 Hz for 40 min) in the absence of any STDP stimulation. These recordings served as negative controls (designated 0:0 controls).

To investigate whether a rise of postsynaptic Ca^{2+} concentration is required for induction of t-LTP under our conditions, we applied the Ca^{2+} chelator BAPTA (10 mM, Sigma, Germany) via the patch pipette solution into the recorded postsynaptic neuron. NMDA receptor (R) dependency was tested by application of an NMDAR antagonist (APV 50 µM, DL-2-Amino-5-phosphonopentanoic acid, Tocris, Germany) in the bath solution. The contribution of L-type voltage gated Ca^{2+} channel activation to t-LTP was evaluated with bath applied Nifedipine (25 µM, Sigma, Germany). To interfere with group I metabotropic glutamate receptor (mGluR) signaling we used bath application of either the $mGlu_1$ receptor antagonist YM298198 (1 µM, Tocris, Germany) or the $mGluR_5$ receptor antagonist MPEP (10 µM, Tocris, Germany) alone, or both blocker simultaneously (the substances were bath applied for a minimum of 15 min prior and during STDP recordings). IP3 receptors were blocked by bath application of 2-APB (100 µM, Tocris, Germany, micro-perfusion pump), 2-APB was applied at least 15 min prior t-LTP induction and was present throughout the recordings. Intracellular infusion of ryanodine (100 µM, Tocris, Germany, infusion for 15 min) was used to block ryanodine receptors of internal calcium stores. Where appropriate, respective controls were performed with ACSF or internal solution containing the same final concentration of DMSO as used for the drug containing solution (i.e. solvent controls) using the same perfusion conditions.

We investigated dopaminergic neuromodulation of STDP by bath application of specific antagonists for D1-like (SCH23390, SCH; 10 µM, Sigma) and D2-like dopamine receptors (Sulpiride, Sulp; 10 µM, Sigma, substances were applied for at least 15 min prior STDP recordings). The contribution of BDNF/TrkB signaling was tested by bath application a scavenger of endogenous BDNF (recombinant human TrkB Fc chimera, R&D Systems, Germany). For scavenging of BDNF, slices were pre-incubated for at least 3h with 5µg/ml TrkB-Fc, and subsequent recordings were performed in the presence of 100 ng/ml TrkB-Fc (compare Edelmann et al., 2015). Positive controls were recorded in slices kept under the same regime, but without the addition of TrkB-Fc. To test low repeat t-LTP under conditions of chronic 50% BDNF reduction, we used heterozygous BDNF $^{+/-}$ mice and respective wildtype littermates as described previously (Edelmann et al., 2015).

The contribution of activity-dependent incorporation of GluA1 subunit containing AMPA receptors to expression of low repeat t-LTP was verified by postsynaptic application of Pep1-TGL (100 µM, Tocris, Germany) via the patch pipette solution. To investigate a possible role of GluA2 lacking calcium permeable (cp-) AMPA receptors, we use bath applied NASPM (1-Naphtyl acetyl spermine trihydrochloride, 100 µM, Tocris, Germany) or IEM-1460 (*N*,*N*,*H*,-Trimethyl-5-[(tricyclo[3.3.1.13,7]dec-1-ylmethyl)amino]-1-pentanaminiumbromide hydrobromide, 100 µM, Tocris, Germany).

Data acquisition and Data Analysis

Data were filtered at 3 kHz using a patch clamp amplifier (EPC-8, HEKA, Germany) connected to a LiH8+8 interface and digitized at 10 kHz using PATCHMASTER software (HEKA, Germany). Data analysis was performed with Fitmaster software (HEKA, Germany). All experiments were performed in the current clamp mode, except for paired pulse ratio (PPR) that was recorded in the voltage clamp mode at -70 mV holding potential, and AMPA/NMDA receptor current ratios that were recorded in voltage clamp at -70 mV and -20 mV holding potential. The holding potential for recording of NMDAR currents was set to the maximal depolarized value (i.e. -20mV) that allow stable

recordings in spite of activated voltage gated K^+ currents. We did not replace K^+ for Cs^+ in our internal solutions, since we wanted to elicit LTP under physiological conditions and AMPAR/NMDAR current ratio had to be measured before and 30 min after t-LTP induction. Input resistance was monitored by hyperpolarizing current steps (250 ms; 20 pA), elicited prior to evoked EPSP responses. The average slope calculated from 10 min control recording (baseline) were set to 100% and all subsequent EPSP slopes of a cell were expressed as percentage of baseline slopes. Synaptic strength was calculated from the mean EPSP slopes 20-30 min (or 50-60 min) after STDP induction, divided by the mean EPSP slope measured during 10 min before STDP stimulation (baseline). Spike timing intervals (i.e. *Δt,* ms) were measured as the time between onset of the evoked EPSP and the peak of the first action potential. Cells were only included for analysis if the initial resting membrane potential (RMP) was between -55 and -70 mV. Cells were excluded when the input resistance varied more than 25% over the entire experiment. Furthermore, traces showing visible “run-up” or “run-down” during baseline recording were excluded. Data were binned at 1 min intervals.

AMPA/NMDA receptor mediated current ratios were calculated from the peak current amplitudes of the fast AMPA receptor mediated components evoked at a holding potential of -70 mV divided by the amplitudes of the NMDAR mediated slow current components measured after 50 ms of the onset of the EPSCs at a holding potential of -20 mV. Selectivity of this procedure for AMPAR and NMDAR mediated currents was confirmed by bath application of either 50 µM APV or 10 µM NBQX in selected experiments (compare Edelmann et al., 2015).

For analysis of presynaptic short-term plasticity before and after t-LTP induction, paired pulse facilitation was recorded in voltage clamp mode at a holding potential of -70 mV, and the paired pulse ratio (PPR) was determined by dividing the peak current amplitudes of the second EPSC by the first EPSC at an inter-stimulus interval of 50 ms.

To further check for a presynaptic LTP expression locus of the 6x 1:1 t-LTP, coefficient of variance (CV) analysis was performed. CV is expressed as standard deviation/mean (Faber and Korn, 1991). The ratio of CV^2 before and after the pairing (20-30 min after induction) was plotted against the respective ratio of mean EPSP slopes (EPSP after/EPSP baseline, Malinow and Tsien, 1990; Manabe et

al., 1993). CV^2 ratio was calculated by dividing $1/CV^2$ after LTP with $1/CV^2$ of baseline. Presynaptic LTP is supposed to influence CV^2 more strongly than the EPSP amplitude so that values lie on or above the diagonal line of unity (Bender et al., 2009; compare Edelmann et al., 2015). As an additional measure for possible t-LTP induced presynaptic changes, putative miniature synaptic currents ("miniature" EPSCs; cut-off amplitude: 15pA to minimize analyses of evoked responses) were analyzed with the Minianalysis program (Synaptosoft, USA) from 3 min of continuous recordings before and 30 min after t-LTP induction. Cumulative fraction plots for amplitudes and inter-event intervals (IEI) were generated. TTX was omitted when recording mEPSCs to allow STDP induction under physiological conditions.

To verify independent expression of the two low repeat paradigms, we performed an occlusion approach. Here we subsequently induced first 6 x 1:1 t-LTP and 25 min later the 6 x 1:4 t-LTP in the same cell and compared the change in synaptic strength by the two protocols.

To assure reproducibility of results, data for experiments shown in **Figs. 1, 3, 5, 8** and **S1** were pooled from 2 or 3 independent experimenters, blind to the results of the other(s).

Statistics

Statistical analysis was performed using GraphPad Prism version 6.0 (GraphPad Software, USA) or JMP 8 (SAS Institute Inc., USA). Pooled data of experiments from at least three different animals are expressed as mean ± SEM. Paired and unpaired two tailed t-tests were used for data with normal distribution. Otherwise nonparametric Mann-Whitney U-test was applied. Multiple comparisons were assessed with a one-way analysis of variance (ANOVA), followed by a post hoc t-test Dunnet's test, or Kruskal-Wallis test, followed by post hoc Dunn's test for parametric and nonparametric data. A p-value <0.05 was set as level of significance and is indicated by an asterisk. The actual statistic procedures used for each experiment are mentioned in the text. The respective number of experiments (n) and the number of animals (N) is reported in the figure legends.

Acknowledgments:

The project was funded by the federal state of Saxony-Anhalt and the "European Regional Developmental Fund (ERDF 2014-2020), Project: Center for Behavioral Brain Sciences (CBBS) FKS: ZS/2016/04/78113; by the federal state Saxony-Anhalt and the European Structural and Investment Funds (ESF, 2014-2020), project number ZS/2016/08/80645 and by the DFG ED 280/1-1 and SFB779/B06. The authors thank Regina Ziegler for excellent technical assistance.

CRediT

Conceptualization: VL, EE; Methodology: VL, EE and EC-P; Investigation: EC-P, BK, GQ, SB with help by EE; Writing: EE, VL, with help by EC-P; Funding Acquisition: VL, EE; Resources: VL; Supervision: VL, EE.

The authors declare no competing interests.

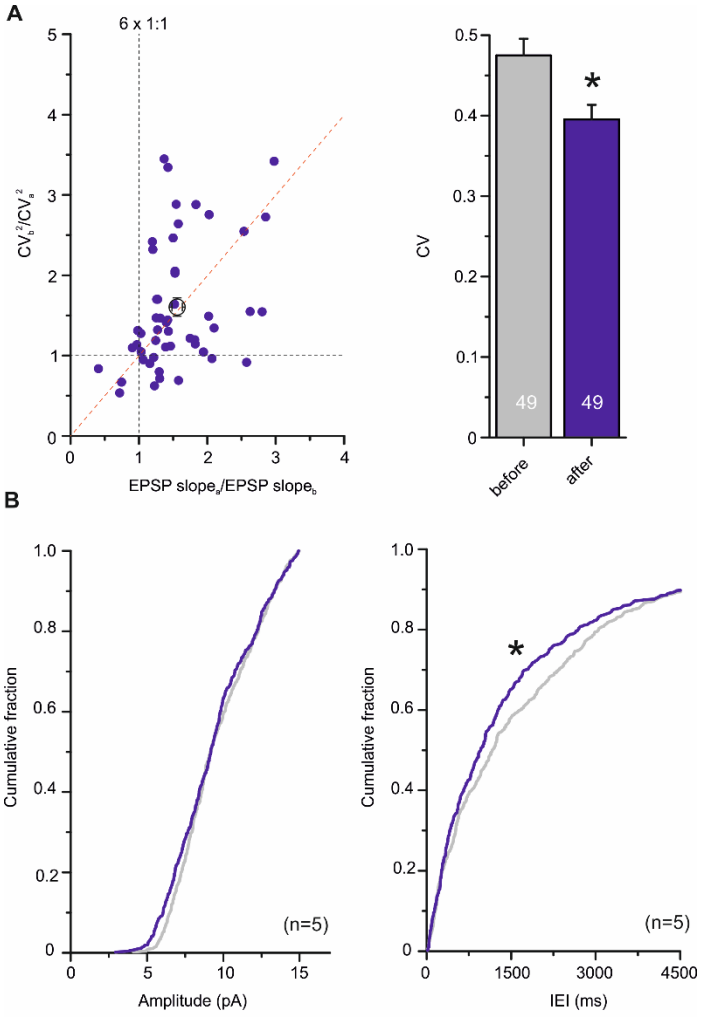

Figure S1: Evidence for presynaptic expression locus of 6 x 1:1 t-LTP. A*) CV^2 analysis. Left: Each point represents an individual cell subjected to 6 x 1:1 t-LTP stimulation. X-axis: magnitude of potentiation; y-axis: change in coefficient of variation. All points on or above the diagonal red line indicate presynaptic expression of 6x 1:1 t-LTP in the respective cell. Right: the average over all cells revealed a significant decrease of CV after t-LTP induction, being consistent with a presynaptic change.* ***B****) Cumulative fraction of mEPSC amplitudes (left) and interevent intervals (IEI; right) before and after 6 x 1:1 t-LTP induction. Blue color indicates cumulative probability after t-LTP induction (grey line: before t-LTP induction). The decrease in IEI (reflecting increased mEPSC frequencies) in the absence of change in mEPSC amplitudes (left) is consistent with a presynaptic change. Data are expressed as mean ± SEM. The analysis shows the results from 49 cells (in A) and 5 cells (B) from at least 3 different animals.*

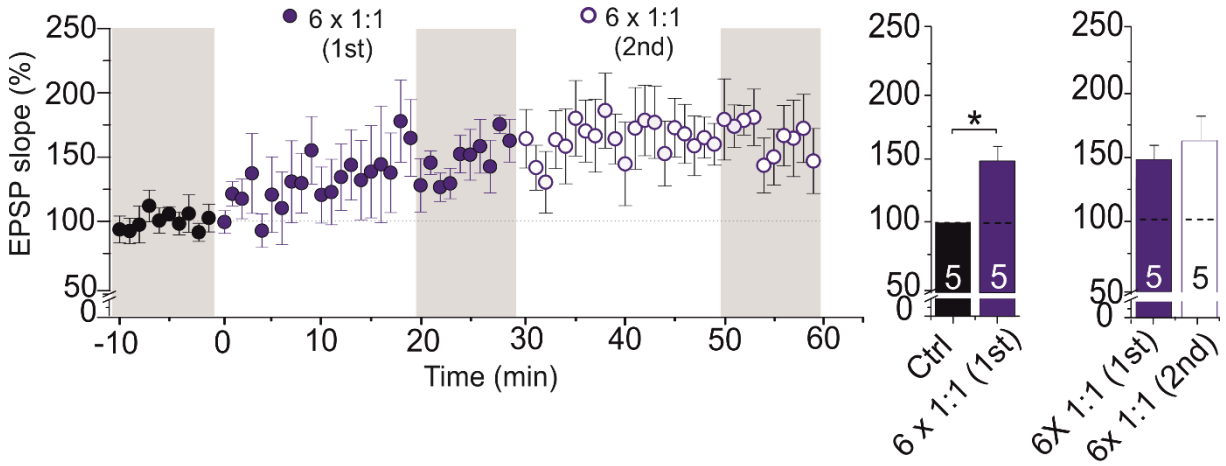

Figure S2: Two subsequent stimulations with the 6 x 1:1 t-LTP protocol do not yield additional potentiation. *SC-CA1 synapses were recorded as in* ***figure 8****, and 6 x 1:1 t-LTP stimulation was performed at 0 and 30 min in the same cells (n=5 / N= 3). The second induction protocol did not significantly increase the magnitude of t-LTP that was reached after the first t-LTP induction. Note that subsequent stimulations with the 6x 1:1 protocol followed by the 6 x 1:4 protocol in the same cells yielded additional and independent potentiation (compare* ***Fig. 8****). Average time course of potentiation and mean (± SEM) magnitude of t-LTP are shown for the respective experiments.*

References

Artola, A., and Singer, W. (1993). Long-term depression of excitatory synaptic transmission and its relationship to long-term potentiation. Trends Neurosci 16, 480-487.

Balkowiec, A., and Katz, D.M. (2002). Cellular mechanisms regulating activity-dependent release of native brain-derived neurotrophic factor from hippocampal neurons. J Neurosci 22, 10399-10407.

Balschun, D., Manahan-Vaughan, D., Wagner, T., Behnisch, T., Reymann, K.G., and Wetzel, W. (1999). A specific role for group I mGluRs in hippocampal LTP and hippocampus-dependent spatial learning. Learn Memory 6, 138-152.

Banerjee, A., Meredith, R.M., Rodriguez-Moreno, A., Mierau, S.B., Auberson, Y.P., and Paulsen, O. (2009). Double dissociation of spike timing-dependent potentiation and depression by subunit-preferring NMDA receptor antagonists in mouse barrel cortex. Cereb Cortex 19, 2959-2969.

Beaulieu, J.M., and Gainetdinov, R.R. (2011). The physiology, signaling, and pharmacology of dopamine receptors. Pharmacol Rev 63, 182-217.

Bender, V.A., Bender, K.J., Brasier, D.J., and Feldman, D.E. (2006). Two coincidence detectors for spike timing-dependent plasticity in somatosensory cortex. J Neurosci 26, 4166-4177.

Bender, V.A., Pugh, J.R., and Jahr, C.E. (2009). Presynaptically expressed long-term potentiation increases multivesicular release at parallel fiber synapses. J Neurosci 29, 10974-10978.

Bi, G.Q., and Poo, M.M. (1998). Synaptic modifications in cultured hippocampal neurons: dependence on spike timing, synaptic strength, and postsynaptic cell type. J Neurosci 18, 10464-10472.

Bi, G.Q., and Poo, M.M. (2001). Synaptic modification by correlated activity: Hebb's postulate revisited. Annu Rev Neurosci 24, 139-166.

Bittner, K.C., Grienberger, C., Vaidya, S.P., Milstein, A.D., Macklin, J.J., Suh, J., Tonegawa, S., and Magee, J.C. (2015). Conjunctive input processing drives feature selectivity in hippocampal CA1 neurons. Nat Neurosci 18, 1133-1142.

Bittner, K.C., Milstein, A.D., Grienberger, C., Romani, S., and Magee, J.C. (2017). Behavioral time scale synaptic plasticity underlies CA1 place fields. Science 357, 1033-1036.

Bliss, T.V., and Cooke, S.F. (2011). Long-term potentiation and long-term depression: a clinical perspective. Clinics (Sao Paulo) 66 Suppl 1, 3-17.

Bliss, T.V., and Lomo, T. (1973). Long-lasting potentiation of synaptic transmission in the dentate area of the anaesthetized rabbit following stimulation of the perforant path. J Physiol 232, 331-356.

Brigadski T, Lichtenecker, P., Lessmann, V. (2019) Recording activity-dependent release of BDNF from hippocampal neurons. Neuromethods book Brain-derived neurotrophic factor (BDNF). Edited by Carlos B. Duarte, Enrico Tongiorgi (143)

Brzosko, Z., Schultz, W., and Paulsen, O. (2015). Retroactive modulation of spike timing-dependent plasticity by dopamine. Elife 4.

Buchanan, K.A., and Mellor, J.R. (2007). The development of synaptic plasticity induction rules and the requirement for postsynaptic spikes in rat hippocampal CA1 pyramidal neurones. J Physiol 585, 429-445.

Caporale, N., and Dan, Y. (2008). Spike timing-dependent plasticity: a Hebbian learning rule. Annu Rev Neurosci 31, 25-46.

Carlisle, H.J., Fink, A.E., Grant, S.G., and O'Dell, T.J. (2008). Opposing effects of PSD-93 and PSD-95 on long-term potentiation and spike timing-dependent plasticity. J Physiol 586, 5885-5900.

1056 Cassenaer, S., and Laurent, G. (2012). Conditional modulation of spike-timing-dependent plasticity
1057 for olfactory learning. Nature 482, 47-52.

1058 Chater, T.E., and Goda, Y. (2014). The role of AMPA receptors in postsynaptic mechanisms of synaptic
1059 plasticity. Front Cell Neurosci 8, 401.

1060 Costa, R.P., Mizusaki, B.E., Sjostrom, P.J., and van Rossum, M.C. (2017). Functional consequences of
1061 pre- and postsynaptic expression of synaptic plasticity. Philos Trans R Soc Lond B Biol Sci 372.

1062 Couey, J.J., Meredith, R.M., Spijker, S., Poorthuis, R.B., Smit, A.B., Brussaard, A.B., and Mansvelder,
1063 H.D. (2007). Distributed network actions by nicotine increase the threshold for spike-timing-
1064 dependent plasticity in prefrontal cortex. Neuron 54, 73-87.

1065 Cui, Y., Paille, V., Xu, H., Genet, S., Delord, B., Fino, E., Berry, H., and Venance, L. (2015).
1066 Endocannabinoids mediate bidirectional striatal spike-timing dependent plasticity. J Physiol.

1067 Cui, Y., Prokin, I., Xu, H., Delord, B., Genet, S., Venance, L., and Berry, H. (2016). Endocannabinoid
1068 dynamics gate spike-timing dependent depression and potentiation. Elife 5, e13185.

1069 Debanne, D., Gahwiler, B.H., and Thompson, S.M. (1998). Long-term synaptic plasticity between pairs
1070 of individual CA3 pyramidal cells in rat hippocampal slice cultures. J Physiol 507 (Pt 1), 237-247.

1071 Drew, P.J., and Abbott, L.F. (2006). Extending the effects of spike-timing-dependent plasticity to
1072 behavioral timescales. Proc Natl Acad Sci U S A 103, 8876-8881.

1073 Dubovyk, V., and Manahan-Vaughan, D. (2018). Less means more: The magnitude of synaptic
1074 plasticity along the hippocampal dorso-ventral axis is inversely related to the expression levels of
1075 plasticity-related neurotransmitter receptors. Hippocampus 28, 136-150.

1076 Dubovyk, V., and Manahan-Vaughan, D. (2019). Gradient of Expression of Dopamine D2 Receptors
1077 Along the Dorso-Ventral Axis of the Hippocampus. Front Synaptic Neurosci 11, 28.

1078 Dudman, J.T., Tsay, D., and Siegelbaum, S.A. (2007). A role for synaptic inputs at distal dendrites:
1079 instructive signals for hippocampal long-term plasticity. Neuron 56, 866-879.

1080 Edelmann, E., Cepeda-Prado, E., Franck, M., Lichtenecker, P., Brigadski, T., and Lessmann, V. (2015).
1081 Theta Burst Firing Recruits BDNF Release and Signaling in Postsynaptic CA1 Neurons in Spike-Timing-
1082 Dependent LTP. Neuron 86, 1041-1054.

1083 Edelmann, E., Cepeda-Prado, E., and Lessmann, V. (2017). Coexistence of Multiple Types of Synaptic
1084 Plasticity in Individual Hippocampal CA1 Pyramidal Neurons. Front Synaptic Neurosci 9, 7.

1085 Edelmann, E., and Lessmann, V. (2011). Dopamine Modulates Spike Timing-Dependent Plasticity and
1086 Action Potential Properties in CA1 Pyramidal Neurons of Acute Rat Hippocampal Slices. Front
1087 Synaptic Neurosci 3, 6.

1088 Edelmann, E., and Lessmann, V. (2013). Dopamine regulates intrinsic excitability thereby gating
1089 successful induction of spike timing-dependent plasticity in CA1 of the hippocampus. Front Neurosci
1090 7, 25.

1091 Edelmann, E., and Lessmann, V. (2018). Dopaminergic innervation and modulation of hippocampal
1092 networks. Cell Tissue Res 373, 711-727.

1093 Edelmann, E., Lessmann, V., and Brigadski, T. (2014). Pre- and postsynaptic twists in BDNF secretion
1094 and action in synaptic plasticity. Neuropharmacology 76 Pt C, 610-627.

1095 Endres, T., and Lessmann, V. (2012). Age-dependent deficits in fear learning in heterozygous BDNF
1096 knock-out mice. Learn Mem 19, 561-570.

1097 Faber, D.S., and Korn, H. (1991). Applicability of the coefficient of variation method for analyzing
1098 synaptic plasticity. Biophys J 60, 1288-1294.

1099 Feldman, D.E. (2000). Timing-based LTP and LTD at vertical inputs to layer II/III pyramidal cells in rat
1100 barrel cortex. Neuron 27, 45-56.

1101 Feldman, D.E. (2012). The spike-timing dependence of plasticity. Neuron 75, 556-571.

1102 Fino, E., and Venance, L. (2010). Spike-timing dependent plasticity in the striatum. Front Synaptic
1103 Neurosci 2, 6.

1104 Froemke, R.C., Tsay, I.A., Raad, M., Long, J.D., and Dan, Y. (2006). Contribution of individual spikes in
1105 burst-induced long-term synaptic modification. J Neurophysiol 95, 1620-1629.

1106 Gao, J., Voss, A.A., Pessah, I.N., Lauer, F.T., Penning, T.M., and Burchiel, S.W. (2005). Ryanodine
1107 receptor-mediated rapid increase in intracellular calcium induced by 7,8-benzo(a)pyrene quinone in
1108 human and murine leukocytes. Toxicol Sci 87, 419-426.

1109 Gerstner, W., Lehmann, M., Liakoni, V., Corneil, D., and Brea, J. (2018). Eligibility Traces and Plasticity
1110 on Behavioral Time Scales: Experimental Support of NeoHebbian Three-Factor Learning Rules. Front
1111 Neural Circuits 12, 53.

1112 Gottmann, K., Mittmann, T., and Lessmann, V. (2009). BDNF signaling in the formation, maturation
1113 and plasticity of glutamatergic and GABAergic synapses. Exp Brain Res 199, 203-234.

1114 Granger, A.J., and Nicoll, R.A. (2014). Expression mechanisms underlying long-term potentiation: a
1115 postsynaptic view, 10 years on. Philos T R Soc B 369.

1116 Hagena, H., and Manahan-Vaughan, D. (2016). Dopamine D1/D5, But not D2/D3, Receptor
1117 Dependency of Synaptic Plasticity at Hippocampal Mossy Fiber Synapses that Is Enabled by Patterned
1118 Afferent Stimulation, or Spatial Learning. Front Synaptic Neurosci 8, 31.

1119 Hayashi, Y., Shi, S.H., Esteban, J.A., Piccini, A., Poncer, J.C., and Malinow, R. (2000). Driving AMPA
1120 receptors into synapses by LTP and CaMKII: requirement for GluR1 and PDZ domain interaction.
1121 Science 287, 2262-2267.

1122 He, K., Huertas, M., Hong, S.Z., Tie, X., Hell, J.W., Shouval, H., and Kirkwood, A. (2015). Distinct
1123 Eligibility Traces for LTP and LTD in Cortical Synapses. Neuron 88, 528-538.

1124 Herring, B.E., and Nicoll, R.A. (2016). Long-Term Potentiation: From CaMKII to AMPA Receptor
1125 Trafficking. Annu Rev Physiol 78, 351-365.

1126 Jong, Y.J., Sergin, I., Purgert, C.A., and O'Malley, K.L. (2014). Location-dependent signaling of the
1127 group 1 metabotropic glutamate receptor mGlu5. Mol Pharmacol 86, 774-785.

1128 Kaar, A., and Rae, M.G. (2015). Metabotropic glutamate receptor-mediated cyclic ADP ribose
1129 signalling. Biochem Soc Trans 43, 405-409.

1130 Kauer, J.A., and Malenka, R.C. (2006). LTP: AMPA receptors trading places. Nat Neurosci 9, 593-594.

1131 Korte, M., Carroll, P., Wolf, E., Brem, G., Thoenen, H., and Bonhoeffer, T. (1995). Hippocampal long-
1132 term potentiation is impaired in mice lacking brain-derived neurotrophic factor. Proc Natl Acad Sci U
1133 S A 92, 8856-8860.

1134 Lalanne, T., Oyrer, J., Farrant, M., and Sjostrom, P.J. (2018). Synapse Type-Dependent Expression of
1135 Calcium-Permeable AMPA Receptors. Front Synaptic Neurosci 10, 34.

1136 Lee, H.K., and Kirkwood, A. (2011). AMPA receptor regulation during synaptic plasticity in
1137 hippocampus and neocortex. Semin Cell Dev Biol 22, 514-520.

1138 Lessmann, V., Gottmann, K., and Malcangio, M. (2003). Neurotrophin secretion: current facts and
1139 future prospects. Prog Neurobiol 69, 341-374.

1140 Lisman, J. (1989). A mechanism for the Hebb and the anti-Hebb processes underlying learning and
1141 memory. Proc Natl Acad Sci U S A 86, 9574-9578.

1142 Liu, Y., Cui, L., Schwarz, M.K., Dong, Y., and Schluter, O.M. (2017). Adrenergic Gate Release for Spike
1143 Timing-Dependent Synaptic Potentiation. Neuron 93, 394-408.

1144 Lu, H., Park, H., and Poo, M.M. (2014). Spike-timing-dependent BDNF secretion and synaptic
1145 plasticity. Philos Trans R Soc Lond B Biol Sci 369, 20130132.

1146 Lynch, M.A. (2004). Long-term potentiation and memory. Physiol Rev 84, 87-136.

1147 Magee, J.C., and Johnston, D. (1997). A synaptically controlled, associative signal for Hebbian
1148 plasticity in hippocampal neurons. Science 275, 209-213.

1149 Malenka, R.C., and Bear, M.F. (2004). LTP and LTD: an embarrassment of riches. Neuron 44, 5-21.

1150 Malinow, R., and Tsien, R.W. (1990). Presynaptic enhancement shown by whole-cell recordings of
1151 long-term potentiation in hippocampal slices. Nature 346, 177-180.

1152 Man, H.Y. (2011). GluA2-lacking, calcium-permeable AMPA receptors--inducers of plasticity? Curr
1153 Opin Neurobiol 21, 291-298.

1154 Manabe, T., Wyllie, D.J., Perkel, D.J., and Nicoll, R.A. (1993). Modulation of synaptic transmission and
1155 long-term potentiation: effects on paired pulse facilitation and EPSC variance in the CA1 region of the
1156 hippocampus. J Neurophysiol 70, 1451-1459.

1157 Markram, H., Gerstner, W., and Sjostrom, P.J. (2011). A history of spike-timing-dependent plasticity.
1158 Front Synaptic Neurosci 3, 4.

1159 Meis, S., Endres, T., and Lessmann, V. (2012). Postsynaptic BDNF signalling regulates long-term
1160 potentiation at thalamo-amygdala afferents. J Physiol 590, 193-208.

1161 Meredith, R.M., Floyer-Lea, A.M., and Paulsen, O. (2003). Maturation of long-term potentiation
1162 induction rules in rodent hippocampus: role of GABAergic inhibition. J Neurosci 23, 11142-11146.

1163 Missale, C., Nash, S.R., Robinson, S.W., Jaber, M., and Caron, M.G. (1998). Dopamine receptors: from
1164 structure to function. Physiol Rev 78, 189-225.

1165 Morita, D., Rah, J.C., and Isaac, J.T. (2014). Incorporation of inwardly rectifying AMPA receptors at
1166 silent synapses during hippocampal long-term potentiation. Philos Trans R Soc Lond B Biol Sci 369,
1167 20130156.

1168 Mu, Y., and Poo, M.M. (2006). Spike timing-dependent LTP/LTD mediates visual experience-
1169 dependent plasticity in a developing retinotectal system. Neuron 50, 115-125.

1170 Nanou, E., Scheuer, T., and Catterall, W.A. (2016). Calcium sensor regulation of the CaV2.1 Ca2+
1171 channel contributes to long-term potentiation and spatial learning. Proc Natl Acad Sci U S A 113,
1172 13209-13214.

1173 Nevian, T., and Sakmann, B. (2006). Spine Ca2+ signaling in spike-timing-dependent plasticity. J
1174 Neurosci 26, 11001-11013.

1175 Neyman, S., and Manahan-Vaughan, D. (2008). Metabotropic glutamate receptor 1 (mGluR1) and 5
1176 (mGluR5) regulate late phases of LTP and LTD in the hippocampal CA1 region in vitro. Eur J Neurosci
1177 27, 1345-1352.

1178 Nicoll, R.A. (2003). Expression mechanisms underlying long-term potentiation: a postsynaptic view.
1179 Philos T R Soc B 358, 721-726.

1180 Nicoll, R.A., and Malenka, R.C. (1995). Contrasting properties of two forms of long-term potentiation
1181 in the hippocampus. Nature 377, 115-118.

1182 Nyberg, L., Karalija, N., Salami, A., Andersson, M., Wahlin, A., Kaboovand, N., Kohncke, Y., Axelsson,
1183 J., Rieckmann, A., Papenberg, G.*, et al.* (2016). Dopamine D2 receptor availability is linked to
1184 hippocampal-caudate functional connectivity and episodic memory. Proc Natl Acad Sci U S A 113,
1185 7918-7923.

Otmakhov, N., and Lisman, J.E. (2002). Postsynaptic application of a cAMP analogue reverses long-term potentiation in hippocampal CA1 pyramidal neurons. J Neurophysiol 87, 3018-3032.

Otmakhova, N.A., Otmakhov, N., Mortenson, L.H., and Lisman, J.E. (2000). Inhibition of the cAMP pathway decreases early long-term potentiation at CA1 hippocampal synapses. J Neurosci 20, 4446-4451.

Otto, T., Eichenbaum, H., Wiener, S.I., and Wible, C.G. (1991). Learning-related patterns of CA1 spike trains parallel stimulation parameters optimal for inducing hippocampal long-term potentiation. Hippocampus 1, 181-192.

Papaleonidopoulos, V., Kouvaros, S., and Papatheodoropoulos, C. (2018). Effects of endogenous and exogenous D1/D5 dopamine receptor activation on LTP in ventral and dorsal CA1 hippocampal synapses. Synapse 72, e22033.

Park, H., and Poo, M.M. (2013). Neurotrophin regulation of neural circuit development and function. Nat Rev Neurosci 14, 7-23.

Park, P., Kang, H., Sanderson, T.M., Bortolotto, Z.A., Georgiou, J., Zhuo, M., Kaang, B.K., and Collingridge, G.L. (2018). The Role of Calcium-Permeable AMPARs in Long-Term Potentiation at Principal Neurons in the Rodent Hippocampus. Front Synaptic Neurosci 10, 42.

Pattwell, S.S., Bath, K.G., Perez-Castro, R., Lee, F.S., Chao, M.V., and Ninan, I. (2012). The BDNF Val66Met Polymorphism Impairs Synaptic Transmission and Plasticity in the Infralimbic Medial Prefrontal Cortex. J Neurosci 32, 2410-2421.

Pawlak, V., and Kerr, J.N. (2008). Dopamine receptor activation is required for corticostriatal spike-timing-dependent plasticity. J Neurosci 28, 2435-2446.

Pike, F.G., Meredith, R.M., Olding, A.W., and Paulsen, O. (1999). Rapid report: postsynaptic bursting is essential for 'Hebbian' induction of associative long-term potentiation at excitatory synapses in rat hippocampus. J Physiol 518 (Pt 2), 571-576.

Pinar, C., Fontaine, C.J., Trivino-Paredes, J., Lottenberg, C.P., Gil-Mohapel, J., and Christie, B.R. (2017). Revisiting the flip side: Long-term depression of synaptic efficacy in the hippocampus. Neurosci Biobehav Rev 80, 394-413.

Plant, K., Pelkey, K.A., Bortolotto, Z.A., Morita, D., Terashima, A., McBain, C.J., Collingridge, G.L., and Isaac, J.T. (2006). Transient incorporation of native GluR2-lacking AMPA receptors during hippocampal long-term potentiation. Nat Neurosci 9, 602-604.

Psotta, L., Rockahr, C., Gruss, M., Kirches, E., Braun, K., Lessmann, V., Bock, J., and Endres, T. (2015). Impact of an additional chronic BDNF reduction on learning performance in an Alzheimer mouse model. Front Behav Neurosci 9, 58.

Remy, S., and Spruston, N. (2007). Dendritic spikes induce single-burst long-term potentiation. Proc Natl Acad Sci U S A 104, 17192-17197.

Rosen, Z.B., Cheung, S., and Siegelbaum, S.A. (2015). Midbrain dopamine neurons bidirectionally regulate CA3-CA1 synaptic drive. Nat Neurosci 18, 1763-1771.

Schildt, S., Endres, T., Lessmann, V., and Edelmann, E. (2013). Acute and chronic interference with BDNF/TrkB-signaling impair LTP selectively at mossy fiber synapses in the CA3 region of mouse hippocampus. Neuropharmacology 71, 247-254.

Seol, G.H., Ziburkus, J., Huang, S., Song, L., Kim, I.T., Takamiya, K., Huganir, R.L., Lee, H.K., and Kirkwood, A. (2007). Neuromodulators control the polarity of spike-timing-dependent synaptic plasticity. Neuron 55, 919-929.

Shi, S., Hayashi, Y., Esteban, J.A., and Malinow, R. (2001). Subunit-specific rules governing AMPA receptor trafficking to synapses in hippocampal pyramidal neurons. Cell 105, 331-343.

Shindou, T., Shindou, M., Watanabe, S., and Wickens, J. (2019). A silent eligibility trace enables dopamine-dependent synaptic plasticity for reinforcement learning in the mouse striatum. Eur J Neurosci 49, 726-736.

Sivakumaran, S., Mohajerani, M.H., and Cherubini, E. (2009). At immature mossy-fiber-CA3 synapses, correlated presynaptic and postsynaptic activity persistently enhances GABA release and network excitability via BDNF and cAMP-dependent PKA. J Neurosci 29, 2637-2647.

Sokoloff, P., Diaz, J., Le Foll, B., Guillin, O., Leriche, L., Bezard, E., and Gross, C. (2006). The dopamine D3 receptor: a therapeutic target for the treatment of neuropsychiatric disorders. CNS Neurol Disord Drug Targets 5, 25-43.

Solinas, S.M.G., Edelmann, E., Lessmann, V., and Migliore, M. (2019). A kinetic model for Brain-Derived Neurotrophic Factor mediated spike timing-dependent LTP. PLoS Comput Biol 15, e1006975.

Suzuki, T., Miura, M., Nishimura, K., and Aosaki, T. (2001). Dopamine-dependent synaptic plasticity in the striatal cholinergic interneurons. J Neurosci 21, 6492-6501.

Takechi, H., Eilers, J., and Konnerth, A. (1998). A new class of synaptic response involving calcium release in dendritic spines. Nature 396, 757-760.

Tigaret, C.M., Olivo, V., Sadowski, J., Ashby, M.C., and Mellor, J.R. (2016). Coordinated activation of distinct Ca(2+) sources and metabotropic glutamate receptors encodes Hebbian synaptic plasticity. Nat Commun 7, 10289.

Tonegawa, S., Morrissey, M.D., and Kitamura, T. (2018). The role of engram cells in the systems consolidation of memory. Nat Rev Neurosci 19, 485-498.

Tritsch, N.X., and Sabatini, B.L. (2012). Dopaminergic modulation of synaptic transmission in cortex and striatum. Neuron 76, 33-50.

Wang, H., Ardiles, A.O., Yang, S., Tran, T., Posada-Duque, R., Valdivia, G., Baek, M., Chuang, Y.A., Palacios, A.G., Gallagher, M.*, et al.* (2016). Metabotropic Glutamate Receptors Induce a Form of LTP Controlled by Translation and Arc Signaling in the Hippocampus. J Neurosci 36, 1723-1729.

Wiera, G., Nowak, D., van Hove, I., Dziegiel, P., Moons, L., and Mozrzymas, J.W. (2017). Mechanisms of NMDA Receptor- and Voltage-Gated L-Type Calcium Channel-Dependent Hippocampal LTP Critically Rely on Proteolysis That Is Mediated by Distinct Metalloproteinases. J Neurosci 37, 1240-1256.

Wittenberg, G.M., and Wang, S.S. (2006). Malleability of spike-timing-dependent plasticity at the CA3-CA1 synapse. J Neurosci 26, 6610-6617.

Xu, T.X., and Yao, W.D. (2010). D1 and D2 dopamine receptors in separate circuits cooperate to drive associative long-term potentiation in the prefrontal cortex. Proc Natl Acad Sci U S A 107, 16366-16371.

Yang, K., and Dani, J.A. (2014). Dopamine D1 and D5 receptors modulate spike timing-dependent plasticity at medial perforant path to dentate granule cell synapses. J Neurosci 34, 15888-15897.

Zhang, J.C., Lau, P.M., and Bi, G.Q. (2009). Gain in sensitivity and loss in temporal contrast of STDP by dopaminergic modulation at hippocampal synapses. Proc Natl Acad Sci U S A 106, 13028-13033.